EFFECT OF PARTIAL REMELTING ON MICROSTRUCTURE AND MECHANICAL PROPERTIES OF THIXOFORMED ALUMINIUM ALLOYS

DIANA ANNASUHAH BINTI AZLAN

UNIVERSITI TEKNIKAL MALAYSIA MELAKA

UNIVERSITI TEKNIKAL MALAYSIA MELAKA

2022

EFFECT OF PARTIAL REMELTING ON MICROSTRUCTURE AND MECHANICAL PROPERTIES OF THIXOFORMED ALUMINIUM ALLOYS

This report is submitted in accordance with requirement of the Universiti Teknikal Malaysia Melaka (UTeM) for Bachelor Degree of Manufacturing Engineering (Hons.)

by

DIANA ANNASUHAH BINTI AZLAN

FACULTY OF MANUFACTURING ENGINEERING

2022

DECLARATION

I hereby, declared this report entitled "Effect of partial remelting on microstructure and
mechanical properties of thixoformed magnesium alloys"
is the result of my own research except as cited in reference.

Signature   : ....

Author's Name : DIANA ANNASUHAH BINTI AZLAN

Date   : 21st January 2022

APPROVAL

This report is submitted to the Faculty of Manufacturing Engineering of Universiti Teknikal Malaysia Melaka as a partial fulfilment of the requirement for Degree of Manufacturing Engineering (Hons). The member of the supervisory committee is as follow:

....
(Profesor Madya Ir. Ts. Dr. Mohd Shukor Bin Salleh)

ABSTRAK

Keputusan penyiasatan eksperimen yang dilakukan dengan aloi aluminium LM 21/A308 dibentangkan. Struktur mikro bahan semasa pencairan separa dalam keadaan separa pepejal disiasat daripada proses berbeza yang dialami oleh bahan dan sifatnya dibandingkan. Pembolehubah yang dikaji ialah proses tuangan kacau, proses pembentukan thixo dan pembentukan thixo dengan proses rawatan haba. Bersama-sama dengan analisis mikrostruktur Scanning Electron Microscope (SEM) dan ujian mekanikal telah dilakukan termasuk ujian tegangan dan ujian kekerasan (Vickers). Berdasarkan dapatan eksperimen, didapati bahawa pencairan semula separa juga boleh mengaburkan struktur. Mikroskop Elektron Pengimbasan membenarkan pencirian mikrostruktur untuk menentukan proses tuangan menghasilkan struktur mikro bukan dendritik dengan kelajuan kacau 500 rpm, mikrostruktur pembentukan thixo adalah hampir sferoid dan pembentukan thixo T6 dirawat haba adalah globul sepenuhnya manakala ujian tegangan membolehkan spesimen pembentukan thixo T6 dirawat haba mempunyai nilai Kekuatan Tegangan Muktamad (MPa), Kekuatan Hasil (MPa) dan Pemanjangan hingga Patah (%) yang tertinggi masing-masing sebanyak 258.77 MPa, 134.36 MPa dan 8.93%. Ujian kekerasan menunjukkan bahawa spesimen yang dirawat haba T6 meningkatkan sifat morfologi dengan 128.4 HV disebabkan oleh penghalusan dan pengglobalisasian juzuk mikro struktur dengan struktur bukan dendritik. Kesan positif struktur mikro struktur mengaburkan kesan keliangan negatif terhadap peningkatan harta benda. Adalah dicadangkan bahawa bahan tetulang akan dilepaskan dalam matriks untuk meningkatkan kekerasan, dan kemuluran dengan peratusan tetulang kepada berat yang lebih tinggi. Selain itu, dengan meningkatkan masa kacauan dan kelajuan kacauan juga mampu menambah baik kekuatan bahan.

ABSTRACT

The results of experimental investigations performed with LM 21/A308 aluminium alloy are presented. The microstructure of the material during partial remelting in the semi-solid state is investigated from different processes experienced by the material and the properties are compared. The variables examined were stirred casting process, thixo-forming process and thixo-forming with heat treatment process. Along with microstructural analysis Scanning Electron Microscope (SEM) and the mechanical tests were performed including tensile test and hardness test (Vickers). Based on the experimental findings, it was obtained that partial re-melting can also obscure the structure. Scanning Electron Microscope allows microstructure characterization to determine as-cast process produced a non-dendritic microstructure with 500 rpm stirring speed, thixoformed near- spheroidal microstructure and thixoformed T6 heat treated was fully globule while tensile test allows thixoformed T6 heat treated specimen to have the highest value of Ultimate Tensile Strength (MPa), Yield Strength (MPa) and Elongation to Fracture (%) of 258.77 MPa, 134.36 MPa and 8.93% respectively. The hardness test showed that T6 heat treated specimen improved the morphological properties with 128.4 HV due to the refinement and globularization of structural micro-constituents with non-dendritic structures. The positive effect of structural microstructure obscures the negative porosity effect on property enhancement. It is suggested that reinforcement materials are to be discharged in the matrix to improve the hardness, and ductility with higher reinforcement to weight percentage. In addition, by increasing the stirring time and stirring speed is also able to improve the strength of the material.

DEDICATION

This research is dedicated from me to my family who constantly supported my work and effort to finish this report with amazing results. Specially made for my Ibu, Abby; my Ayah, Azlan; specifically my Syaifullah.

ACKNOWLEDGEMENT

First among all, I would like to thank and give my gratitude to the person who guides me along the way, my supervisor, Profesor Madya Ir. Ts. Dr. Mohd Shukor Bin Salleh. without his time and effort in helping me throughout this research, I surely will not be able to finish it.

Besides that, I would like to thank the technician of FKP Casting Laboratory, Mrs. Zulin, who has spent her time to give her best from the experience and knowledge about my project while doing this project.

Other than that, I want to thank my friends, Ain, Athirah, Afiqah, Afifah, Nabilah, Faizin and Suhailah for giving me the motivation to further this research to the end. Finally, my biggest love and thanks goes to my beloved family who understand me especially my parents, Azlan bin Adnan and Siti Arbaiyah binti Kadir thank you so much.

LIST OF TABLES

LIST OF FIGURES

UNIVERSITI TEKNIKAL MALAYSIA MELAKA

LIST OF ABBREVIATIONS

S.S.M.P	-	Semi-solid Metal Processing
EBSD	-	Electron Backscatter Diffraction
VW	-	Volkswagen
HCP	-	Hexagonal Close-packed
3C	-	Computer, Communication, Consumer
ASTM	-	American Society for Testing Materials
SAE	-	Society of Automotive Engineers
RE	-	Rare Earth
Li	-	Lithium
Al	-	Aluminium
Si	-	Silica
Ca	-	Calcium
Mn	-	Manganese
Cu	-	Copper
Zn	-	Zinc
Sr	-	Strontium
Y	-	Yttrium
Zr	-	Zirconium
Ag	-	Argon
A	-	Aluminium
E	-	Rare Earth
H	-	Thorium

K	-	Potassium
M	-	Manganese
Q	-	Silver
S	-	Silicon
T	-	Tin
Z	-	Zinc
BTU	-	British Thermal Unit
AZ31	-	Aluminium Zinc-based Alloy with 3 and 1 percentile
AS41	-	Aluminium Silicon-based with 4 and 1 percentile
M.I.T	-	Massachusetts Institute of Technology
C.S	-	Cooling Slope
ITT	-	International Telephone and Telegraph
MHD	-	Magnetohydrodynamic
Ti-B	-	Boron Titanium
NRC	-	New Rheocasting
DTM	-	Direct Thermal Method
SCR	-	Shearing-Cooling Roll
SIMA	-	Stress-Induced and Melt-Activated
SEM	-	Scanning Electron Microscope
EDS	-	Energy Disperse Spectroscopy
OM	-	Optical Microscope
XRD	-	X-ray Diffractometer
H2O	-	Water
HNO3	-	Hydrogen Nitrate
CrO3	-	Chromium Trioxide
D	-	Diameter
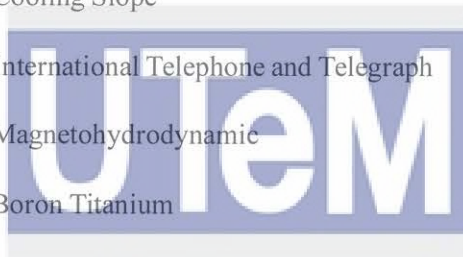
N	-	Total Grain Numbers
F	-	Factor
HV	-	Hardness Vickers
T6	-	Treatment 6

UTeM

اونيۏرسيتي تيڪنيكل مليسيا ملاك

UNIVERSITI TEKNIKAL MALAYSIA MELAKA

LIST OF SYMBOLS

^{0}C   -   Degree Celsius

^{0}F   -   Degree Fahrenheit

%   -   Percentage

GPa   -   Giga Pascal

K^{-1} -   Kelvin power^{-1}

V   -   Voltage

g/cm^3 -   gram per centimetre cube

lb/in^3 -   pound per inch cube

Mpa   -   Mega Pascal

ksi   -   Kilopound per square inch

$\mu m/m^0C$ -   micrometre per metre degree Celsius

W/mK   -   Watt per milli Kelvin

nm   -   nanometre

μm -   micrometre

wt.%   -   weight percentage

mm   -   micrometre

kW   -   kilowatt

g   -   gram
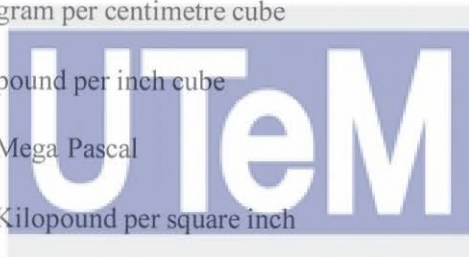
CHAPTER 1.0
INTRODUCTION

1.1 Background of Study

Semi-solid metal processing (S.S.M.P.) is the processing of alloys at temperatures between solidus and liquidus. When thixotropic behaviour was discovered in the early years of 1970 Spencer was supervised by Flemings. They relied on the thixotropic behaviour of metallic alloys at the time. (Spencer et al., 1972). They discovered that implementing shear to alloys as they were solidifying lowered stress. As an outcome, the tension was significantly lower at a temperature just below liquidus than when the alloy was chilled to the same temperature without shearing. (Fan, 2002). The creation of globular microstructures in solid phases is related to the distinctive features of these alloys, surrounded by the homogenously distributed liquid fractions (Riek et al., 1975). Metallic alloy suspensions' qualities were promptly put to use in industries (Mehrabian and Flemings, 1972). The technology consisted of two main operational activities: preparing the globular microstructure and forming a semi-solid slurry. The thixotropic structure was referred to as "rheo-forming" or "thixoforming," depending on how it was produced from the liquid phase directly or from the solid state.

1.2 Problem Statement

Today's industries, after oxygen and silicon, aluminium is the most prevalent mineral on Earth, making it the most widely available metal naturally found on the globe and the second-most consumed metal in the world, just behind iron. Even if the aluminium content is as high as 99 percent, it is primarily employed as an alloy. (Flagel, 2020). However, there are some limitations when using aluminium alloys to perform in semi-solid manufacturing process (S.S.M.P). This is due to the high sensitivity of temperature which impacts the formation of the nucleation and growth of the alloy and reduces bonding between grain

structure during solidification, which decreases formability efficiency during the secondary forming process (Zhu et al., 2004). Through partial remelting of semi-solid metal processing, the desired condition of aluminium alloy slurry can be achieved. The partial remelting process, however, has a state of phase that needs to be analysed. Similar to the cooling slope casting process, there is also a morphological situation to achieve the semi-solid slurry mechanism. In addition, less research are allocated for LM21/A308 aluminium alloy in semi-solid metal processing.

1.3 Objectives

1) To produce aluminium alloy for thixoforming using partial remelting.

2) To investigate the microstructural evolution of aluminium alloy after partial remelting.

3) To determine the mechanical properties of thixoformed aluminium alloy.

1.4 Scope of Project

This study showed microstructure evolution and properties of LM21 aluminium alloy when it underwent the stir casting process before thixoforming and then treated with T6 heat treatment after thixoforming. The outcome measurement of aluminium alloy will be identified by the morphological analysis of which of the process will give non-dendritic structure by scanning electron microscopy while the hardness and tensile tests are for the mechanical properties.

1.5 Significant / Important of Study

There are some potential advantages that can be obtained after the partial re-melting process for industry. The application of structural components for common engineering reasons, LM21 is suited for many of the applications that LM4 can be utilised for. It's typically employed in applications where a large proof stress and rigidity are necessary without the use of heat treatment. Its casting qualities enable it to be employed for the creation of slender forms as well as pressure-tight castings. LM21 can be used for both sand and permanent mould castings. It's utilised in diesel engine crankcases, clutch cases, gear boxes, tool

2

handles, domestic fittings, electrical equipment, and office equipment, among other things. With the addition of this study, limitations of aluminium alloy use can be decreased.

1.6 Organization of the Report

The first chapter gives the overall introduction of my project. Based on the background of the study, the problem statement, objectives, scope of the project, significance of the study, organization of the report and summary of the project.

The second chapter gives the review of Aluminium and Aluminium Alloy, Machinability of Aluminium, Semi Solid Metal Processing (SSMP), Stir Casting, Thixoforming Process and T6 Heat Treatment.

The third chapter gives the flow of methodology used for the whole project starting with the experimental design, preparation of material used, processing, microstructural analysis and mechanical testing.

The fourth chapter discusses the results of the experiment from the microstructural analysis and the mechanical properties analysis.

The last chapter concludes the whole project based on the findings gathered.

1.7 Summary

The aim of this study is to provide the fundamentals of semi-solid metal processing for aluminium alloys. This research focuses on how the microstructure of aluminium alloy varies with different processes to make the semi-solid slurry. Analysis from the process that affects the condition of the microstructure and mechanical properties will be obtained.

CHAPTER 2.0
LITERATURE REVIEW

This chapter discusses literature of aluminium alloy and its properties along with the different processes that will be underwent according to the previous chapter that is under semi-solid metal process. The literature review part is divided into three parts which are Aluminium and Aluminium Alloy, Machinability Aluminium Alloys and Semi-solid Metal Processing.

2.1 Aluminium and Aluminium Alloy

2.1.1 Aluminium

Aluminium is a ductile, malleable, corrosion-resistant metal with a high electrical conductivity. It's commonly used for foil and conductor cables, but it needs to be alloyed with other elements to achieve the greater strengths required for other uses. Aluminium is one of the lightest engineering metals, with a strength-to-weight ratio that is higher than steel.

Aluminium is being used in an ever-increasing variety of applications by combining its beneficial features such as strength, lightweight, corrosion resistance, recyclability, and machinability. This collection of items includes anything from building components to tiny packaging foils. Below in the Table 2.1 is shown the properties of aluminium.

Table 2. 1: Properties of Aluminium (AZOM Materials)

No.	Property	Value / Characteristics
1	Atomic Number	13
2	Atomic Weight (g/mol)	26.98

4

3	Valency	3
4	Crystal Structure	FCC
5	Melting Point (°C)	660.2
6	Boiling Point (°C)	2480
7	Mean Specific Heat (0-100°C) (cal/g.°C)	0.219
8	Thermal Conductivity (0-100°C) (cal/cms. °C)	0.57
9	Co-Efficient of Linear Expansion (0-100°C) (x10^{-6}/°C)	23.5
10	Electrical Resistivity at 20°C (Ω.cm)	2.69
11	Density (g/cm^3)	2.6898
12	Modulus of Elasticity (GPa)	68.3
13	Poissons Ratio	0.34

2.1.2 Aluminium Alloys

Aluminum alloys have a unique combination of low density, formability, excellent thermal and electrical conductivity, high strength-to-weight ratio and corrosion resistance Aluminium alloys are a very relevant material in modern industries due to their characteristics and low production costs. They were used in a variety of industries, such as the automotive, aeronautics, maritime, and electronic industries, as well as food packaging and cans, culinary utensils, construction, and chemical equipment (Wallerstein et al., 2021).

2.1.3 ASTM / SAE Alloy Designation

Aluminium alloys are given a designation according to the ASTM/SAE system which is universally accepted. According to this order, the first two letters point LM to the principles alloying elements, then the next two numbers 21 specify nominal percentage of these alloying elements in the equivalent order and the next capital letter indicates chronological sequence of development. Table 2.2 below shows alloying elements.

5

Table 2. 2: Designations for Elements Alloying (Sameehan, 2016).

Code	Element
A	Aluminium
E	Rare Earth
H	Thorium
K	Zirconium
M	Manganese
Q	Silver
S	Silicon
T	Tin
Z	Zinc

2.1.4 LM21 Aluminium Alloys

LM21 aluminium alloy (Al-Si6Cu4Mn0.4Mg0.2) or A308 is chosen as the matrix material due to their properties such as excellent casting characteristics, better machinability and higher proof strength. The elemental composition of Al LM21 alloy is shown in Table 2.3. This alloy is particularly well suited to castings that needs advanced proof stress and hardness in the as-cast condition, as well as good machinability and formability.

The chemical composition of aluminium LM21 cast alloy is shown in the following table.

Table 2. 3: Chemical Composition of LM21 alloy (Institute Of Technology Tallaght, 2007).

Element	Content (%)
Aluminum, Al	Remainder
Titanium	0.2
Manganese, Mn	0.5
Zinc, Zn	0.2
Silicon, Si	10-13
Copper, Cu	0.4
Lead	0.1
Nickel, Ni	0.1
Others, each max	0.02
Magnesium, Mg	0.2
Tin	0.1

6

2.1.4.2 Physical Properties

The physical properties of the aluminium LM21 cast alloy are shown below in Table 2.4.
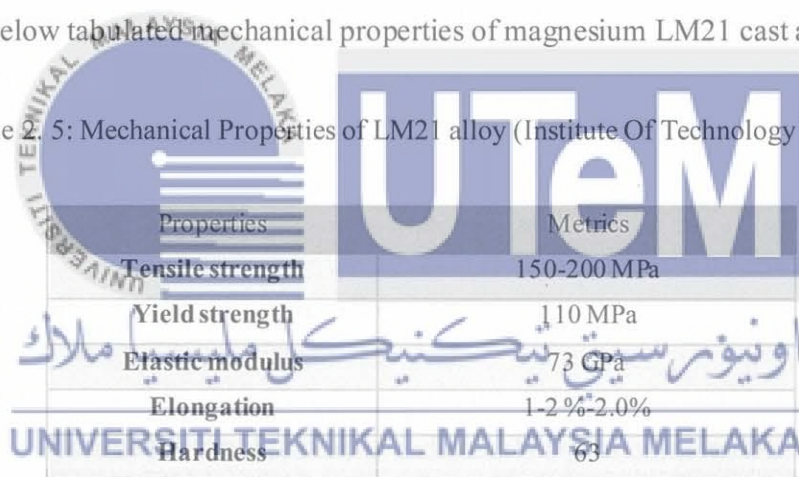
Table 2. 4: Physical Properties of LM21 alloy (Institute Of Technology Tallaght, 2007).

Properties	Metrics
Density	2.81 g/cm^3
Freezing Range	$615\text{-}520^0\text{C}$

2.1.4.3 Mechanical Properties

Table 2.5 below tabulated mechanical properties of magnesium LM21 cast alloy.

Table 2. 5: Mechanical Properties of LM21 alloy (Institute Of Technology Tallaght, 2007).

Properties	Metrics
Tensile strength	150-200 MPa
Yield strength	110 MPa
Elastic modulus	73 GPa
Elongation	1-2 %-2.0%
Hardness	63

2.1.4.4 Thermal Properties

Aluminium LM21 cast alloy with the given thermal properties as in Table 2.6.

Table 2. 6: Thermal Properties of LM21 alloy (Institute Of Technology Tallaght, 2007).

Properties	Metrics
Coefficients of Thermal Expansion (per°C at 20-100°C)	0.000021
Thermal Conductivity (cal/cm2/cm/°C at 25°C)	0.29

2.1.5 Advantages of Aluminium Alloys

1) The lightest metal structure material for engineering application
2) Great specific strength and stiffness
3) Good damping properties
4) Excellent castability
5) Very good machinability and processability
6) Good damping behavior
7) Integrated recycling possible

However, there are some limitations to using aluminium alloys, despite their excellent properties. Aluminium alloys have numbers of drawbacks for machining and processing applications, including poor cold working behavior and low corrosion resistance. Apart from that, when it comes to the application of casting aluminium alloys, they easily solidify and shrink by about 4% to 5% when cooled. This is due to its high reactivity (Kainer, 2003).

2.2 Machinability in Aluminium Alloys

In this segment, we will be reviewing the aluminium alloys machinability rating group. The majority of alloys may be machined easily and quickly than most materials if the machining conditions are chosen to match the features of the numerous alloys. Although machinability is a combination of several qualities, it is feasible to classify alloys based on how effortlessly small, regular chips may be generated on machining with minimal tool wear. An attempt at such classification is given in Table 2.7. The inclusion of copper increases the alloys' machinability. From the table, LM21 is in Group 3 as the second easiest to machine group. LM21 has excellent machinability and outperforms LM4-M in this regard. Tungsten carbide tools are suggested for the best results. It is recommended that the use a lot of cutting lubrication and coolant (Institute Of Technology Tallaght, 2007).

Table 2. 7: Machinability ratings of aluminium casting alloys

Rating group Alloys	Alloys
Group 4	LM5, LM12
Group 3	LM4, LM16, LM21, LM22, LM24, LM25, LM26, LM27, LM31
Group 2	LM0, LM2, LM9, LM13
Group 1	LM6, LM20, LM28, LM29, LM30
NOTE: Alloys in group 4 are easiest to machine, the machinability decreasing through to group 1.	

2.2.3 Applications of LM21 aluminium alloys

Many of the applications for which LM4 can be utilised for basic industrial applications are applicable for LM21. It's typically employed in applications where a high proof stress and rigidity are demanded without the use of heat treatment. Its casting properties allow it to be utilised to make somewhat thin shapes as well as castings that must be pressure tight. LM21 can be used for both sand and permanent mould castings.
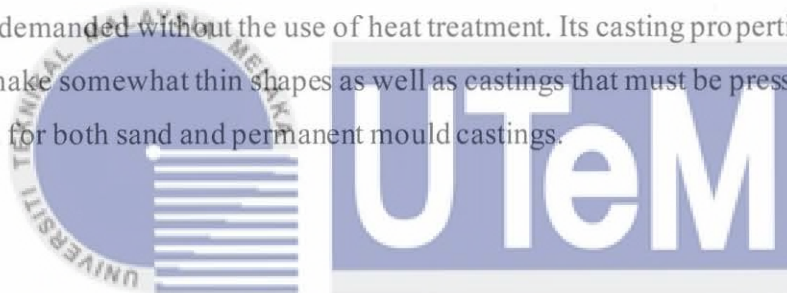
2.3 Semi-solid Metal Processing

2.3.1 Origin of S.S.M.P.

Semi-solid metal processing (S.S.M.P.) began with the encounter of its discovery in the early 1970s, shear thinning and thixotropic types of behaviour of partially solidified alloys were studied under vigorous agitation (Flemings, 1991). Spencer was a postdoctoral fellow at M.I.T. in Cambridge, Massachusetts, under Prof. M. C. Fleming's guidance in 1970s, and was conducting hot tearing tests on a Sn-15 percent Pb alloy. The shearing began above the liquidus temperature during an experiment involving a semisolid alloy viscosity measurement and continued as the slurry slowly cooled through the soppy zone until the solidification process was near completion. The viscosity of the slurry was decreased by shear thinning to the point where it acted like a fluid, preventing dendrite formation and solute segregation (Chang et al., & Kumar et. al). Dendritic material was discovered when it was chilled to a semi-solid condition without stirring as in Figure 2.1(a), while the microstructure of the continuously stirred materials was spheroidal (consisted of spheroids

9

of solid in the liquid matrix) as in Figure 2.1(b). As a result, it was discovered that a semi-solid alloy with a solid fraction of 0.4 and no dendritic structure acts like a fluid with a viscosity lower than olive oil. The viscosity of semisolid alloys subjected to constant agitation during cooling was likewise found to be substantially lower than that discovered when cooling was done without agitation (Flemings, 1991; Fan, 2005 & Atkinson, 2010).
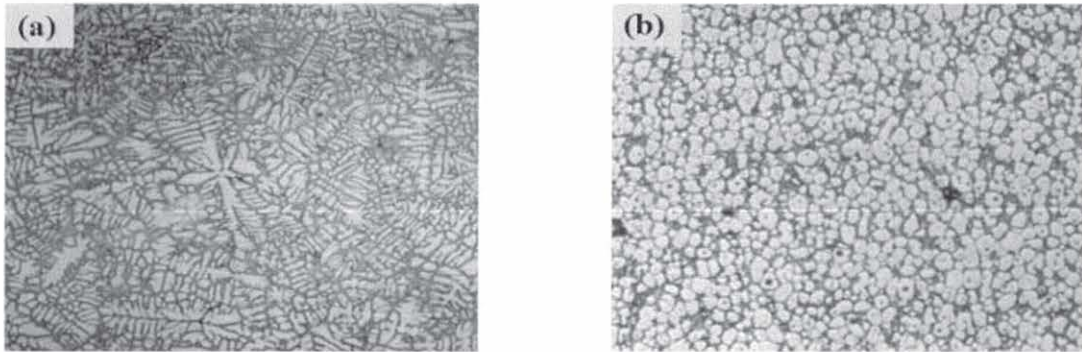
Figure 2.1: (a) Dendritic microstructure (b) Globular microstructure (Atkinson, 2010).

UNIVERSITI TEKNIKAL MALAYSIA MELAKA

2.3.2 Classification of Semi-solid Processing routes

A lot of research and development has gone into investigating the feasibility of S.S.M. processing over the last four decades, and there are a lot of reviews on S.S.M.P. (Kirkwood et al., 1994). Semi-solid processing can be separated into two types: rheo-casting and thixo-casting. Rheo-casting is the method of shearing non-dendritic semi-solid slurry while solidification to produce non-dendritic semi-solid slurry. Rheo-casting was envisioned as a technique incorporating the control of the semisolid alloy's rheological behaviour. (Flemings, 1991). The semisolid alloy is agitated during rheo-casting, which causes dendrites to break up. The method of producing a near net shape from a partially melted non-dendritic alloy slug inside a metal die is known as thixoforming. Thixo-casting refers to the process of moulding a component in a closed die, whereas thixo-forging refers to the process of shaping a component in an open die.

2.3.3 Semi-Solid Slurries and Its Rheological Behaviour

In order to achieve an excellent processing of semi-solid metal, a good understanding of semi-solid slurry is important. The rheological characteristics of semi-solid alloy is the liquidus and solidus range of the flow behaviour. It is stated the behaviour is dependent on temperature and shear rate (Kirkwood, 1994; Fan, 2002). The rheological properties of semi-solid slurry are very important as it will give prediction of flow into die cavities and for that the processing control. There are two categories for the S.S.M. slurries, which are the liquid-like and solid-like phases. Thus, the mechanism of deformation of both slurries is different. The mechanisms are thixotropy and the pseudo-plasticity. Thixotropy occurs when the transient viscosity at a particular shear rate is time dependent, but pseudo-plasticity occurs when the shear rate is dependent on the steady state viscosity (Fan, 2002).

2.3.4 Evolution Practices for Producing Nondendritic Feedstock

As previously stated, a vital step in attaining successful S.S.M processing is providing feedstock with thixotropic characteristics. Furthermore, based on the current state of the beginning material, S.S.M technologies are split into two types : (1) from a liquid alloy via controlled solidification (by activating crystal multiplication of a growing solid or increasing the nucleation rate) under specific conditions, or (2) from a solid state via heavy

11

plastic deformation and recrystallization (Hirt & Kopp, 2009). Over the last 40 years, a variety of feedstock production pathways have been created, each of which is based on the activation of well-known metallurgical occurrences that define the end structure's development (Atkinson, 2007). The most effective, as well as the most widely employed in commercial practise, approaches are briefly outlined here.

2.3.5 Partial Re-melting

Partial re-melting is considered one of the most effective solid-state routes to produce a nondendritic microstructure, especially for high melting point metals when the metal is directly heated to a temperature between solidus and liquidus (Sugiyama et al., 2008Using a vertical, high-temperature carbolite furnace with an argon gas protective environment, a direct partial re-melting experiment was carried out, as shown in Figure 2.2. The specimen (base and insert) was lowered into the highest temperature region (1320°C) of the furnace using chromel wire once the furnace had achieved the predetermined temperature and It was kept around for 30 minutes before being cooled to room temperature with air. This method guarantees a quick heating of the sample, which usually takes around 3 minutes to achieve the desired temperature, as shown in Figure 2.3.
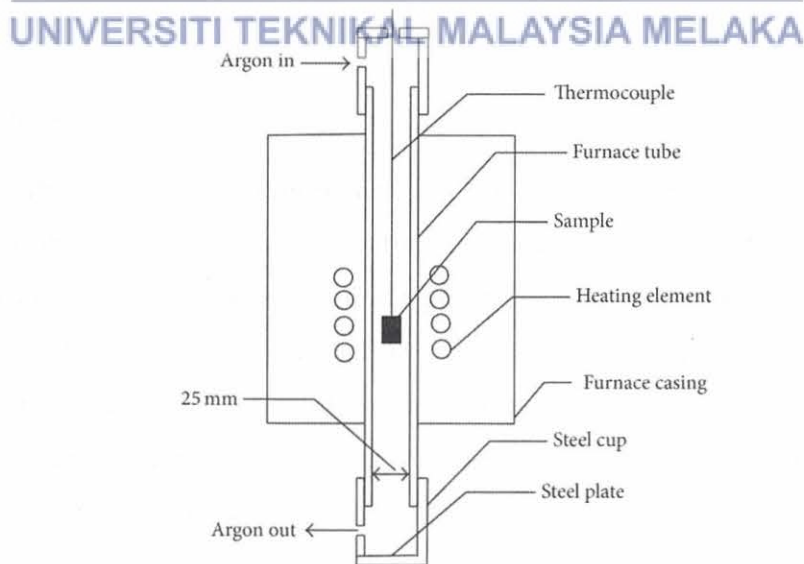
Figure 2. 2: Schematic of the furnace setup for re-melting experiment (Sugiyama et al., 2008).

12
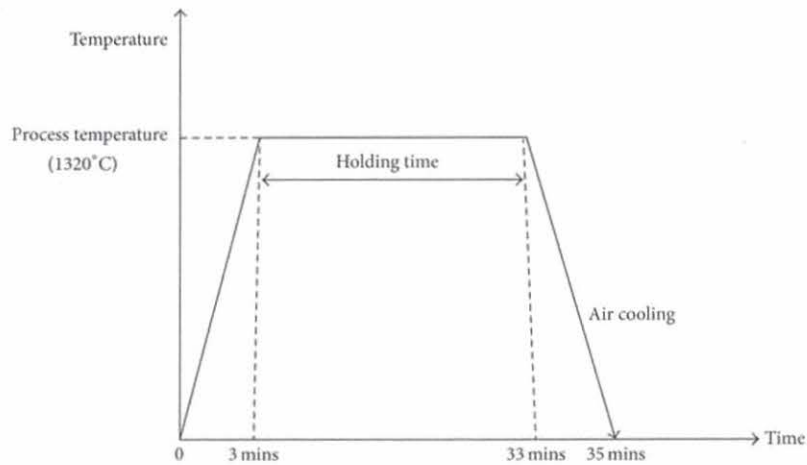
Figure 2. 3: Temperature profile of sample inside vertical tube furnace (Sugiyama et al., 2008).

Direct Partial Re-melting is a method of joining two metals in a thixotropic property (Mohammed, M.N., 2013). This procedure is capable of producing homogenous qualities with a high-quality surface while preventing the formation of a dendritic microstructure in the join zone. In other meanings, because of its high fluidity, a microstructure comprising global solid particles in a liquid matrix has been taken into account the most appropriate microstructure for semi-solid forming (Sugiyama et al., 2008). If the grain boundaries are sufficiently wetted, the initial shear during the forming process may affect the grains to slide past one other, causing the semi-solid slurry to flow thixotropically.

2.3.6 Cooling Slope Casting (C. S)

The high costs related to producing the specialised ingots required for thixoforming that have non-dendritic or globular microstructures are one of the major factors contributing to the increased premiums of the thixoforming process. As a result, research on the growth of feedstock methods has been pursued in recent years, permitting the production of feedstock materials in a more cost-effective manner. The casting process is one of the technologies created to generate feedstock material, and it reduces a significant portion of the prices of thixoformed goods (Haga et al., 2002).

2.3.6.1 C. S Process

Cooling slope casting is a straightforward and concise process that entails pouring molten metal with a suitable superheat through a cooling slope plate and then solidifying in a mould (Haga and Suzuki, 2001). This is a relatively new process for producing raw material for subsequent thixoforming processes. As shown in Figure 2.4, the cooling slope casting process is made up of the following major process sections. A melting pouring section (1), which consists of a crucible which melts the alloy and pours it down through the cooling slope plate. A nucleation section (2), which generates crystal nuclei in the melt as it is flowing through the cooling slope plate. A crystal generating section (3) in which metal obtained from the nucleation section is cooled down in the metal mould.
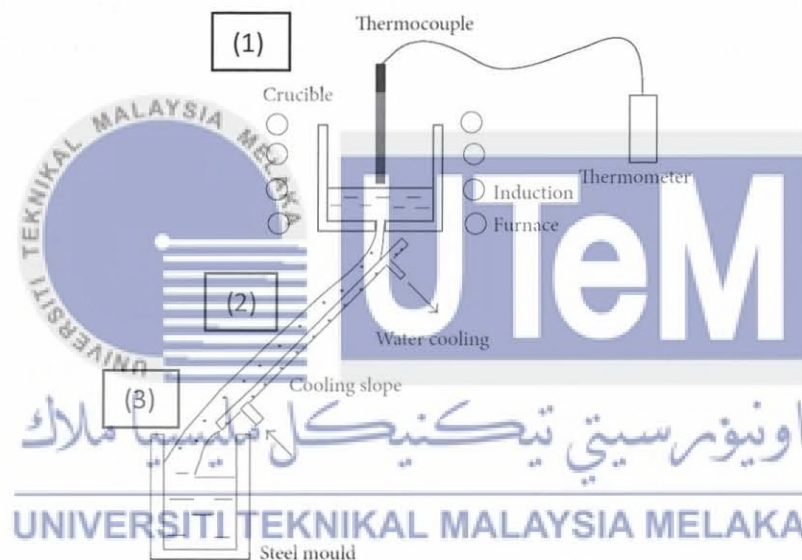
Figure 2. 4: Schematic Process of Cooling Slope Casting with Divided Process Sections; (1), (2) and (3) (Liu et al., 2003).

2.3.6.2 Mechanisms involved in C.S casting process

Few mechanisms have been suggested to describe the formation of non-dendritic microstructures during the flow of the C.S casting process. According to past researchers (Haga and Kapranos, 2002), during the microstructural evolution of C.S. casting, the dendritic fragmentation mechanism played a major role. Fragmentation of weak dendritic arms might occur on the contact surface of cooling slope samples because dendritic crystals in the partially solidified melt meet under gravitational pressures on the inclined slope. These crystals grow in the mould after being formed by the separation of weak dendrite arms along

14

the cooling slope plate using a dendritic fragmentation mechanism. As per Motegi et al. (2007), crystal separation theory is important for the activation of non-dendritic morphology in as-cast C.S microstructures.

Figure 2.5(a) depicts the separation theory mechanism of crystal necking and detachment from mould walls. Granular crystals grow and build on the cooling slope wall before being carried away by fluid velocity, according to this theory. They suspect that metal crystals formed on the cooling plate and were migrated with molten alloy into a heating mould, where they became granular, resulting in a fine globular microstructure (Hirt and Kopp, 2009). As shown in Figure 2.5, Temperature profiles in the liquid containing distinct gradients of solute concentration ahead of the solidification front produce varied growth trends in various locations of the solid surface (b). At higher gradients (roots of the crystal in contact with the cold surface), the deterioration in change temperature is greater, resulting in less boundary undercooling and as a result smaller growth rate.
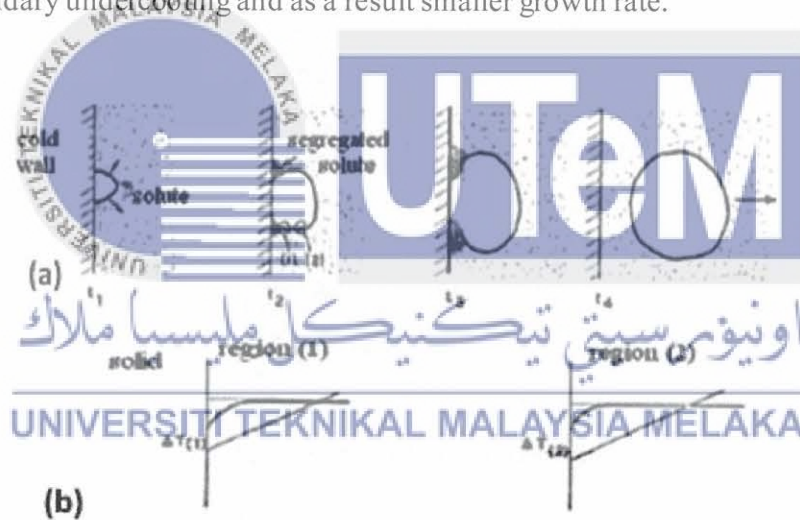
Figure 2. 5: (a) Schematic illustration of crystal separation mechanism of detachment of nuclei from the surface of the cooling .slope (b) temperature profiles in the liquid in the solidification front, for an alloy with partition coefficient (K) < 1 (Robert et al., 2007).

2.3.6.3 Microstructural evolution during flow along the cooling slope

The most important step in semi-solid metal forming innovation is the cost-effective production of semisolid slurry with a non-dendritic microstructure. After remaining in the semisolid state, the primary crystal of the semisolid slurry analysed through the cooling slope

becomes spherical. Solid nuclei are shaped during the process as a result of contact between the melt and the cooling slope, which causes rapid heat transfer. These nuclei separate from the surface and are eventually distributed throughout the melt (Haga et al., 2002; Birol, 2007). Matthias et al. (2010) compared the microstructures of A356 alloy cast conventionally and by cooling slope casting process and found that the latter looks significantly different than the former, even when cooling rates were the same. The morphologies of the A356 alloy produced by this group via conventional casting have a dendritic structure, as shown in Figure 2.6 (a), however those processed via C.S typically have globular grains, as shown in Figure 2.6 (b).
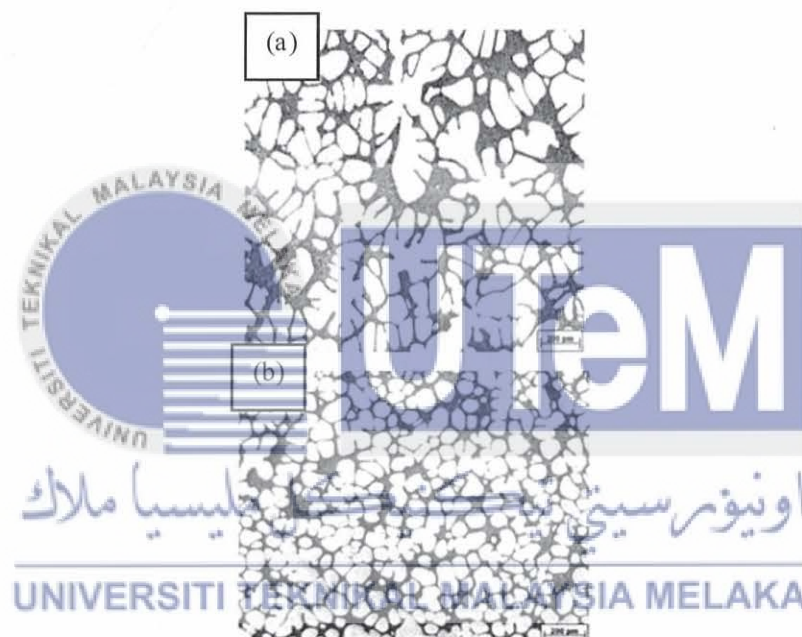
Figure 2. 6: Morphology of A356 Alloy (a) Conventionally cast (b) Cooling Slope Casting (Matthias et al., 2010).

2.3.7 New MIT

The New MIT agitation method is a cross between stirring and near-liquid casting. The procedure, known as the Semisolid Rheo-casting (SSR) process, was established at MIT in 2000. This method of preparing the slurry can be divided into three steps. The first ever step is to hold molten metal a little above its liquidus temperature in order to achieve a uniform temperature slope. Step two is to insert a cool rod (typically made of graphite) into

16

the melt to stir and rapidly chill the metal up until it reaches a temperature that is significantly lower than its liquidous temperature (i.e., to initiate solidification). The final step is to remove the stirrer and either immediately insert the metal into the casting device or slowly cool it to reach the required solid fraction.

As illustrated in Figure 2.8, it can produce globular microstructures (Wan et al., 1994; Figueredo et al., 2001). For such approach, the process of dendritic fragmentation is as described in the following. The cold graphite stirrer is inserted into the liquid metal, and the resulting low superheat temperature triggers the nucleation of numerous fine dendritic grains on the stirrer's surface. These particles are swiftly removed and distributed as very fine grains throughout the melt. These grains are then re-melted due to the surrounding bulk liquid that still has small areas of superheated liquid within it. Upon cooling the melt for a predetermined time, fine grained particles form, resulting in nondendritic microstructures (Motegi et al., 1997). Figure 2.7 depicts a schematic diagram of the microstructure of the 356 alloy achieved by the New MIT process.
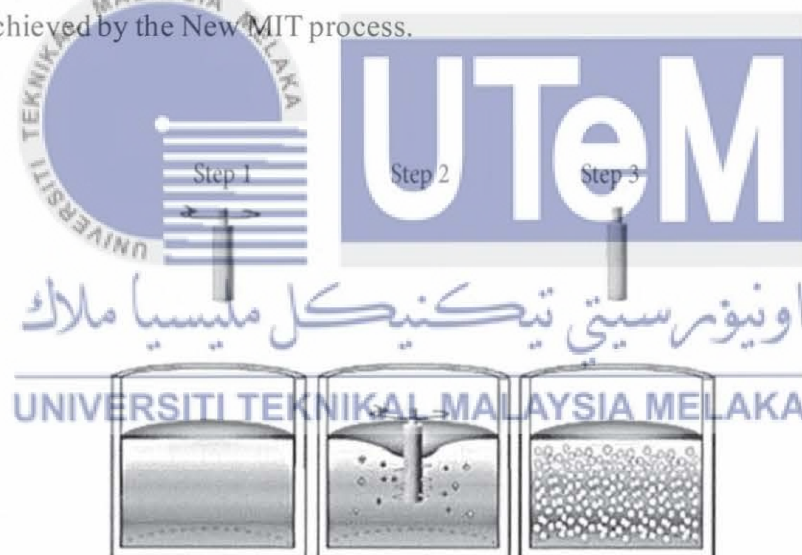
Figure 2. 7: Diagram of the steps of the SSR(Figueredo and Apelian, 2001)

100 μm
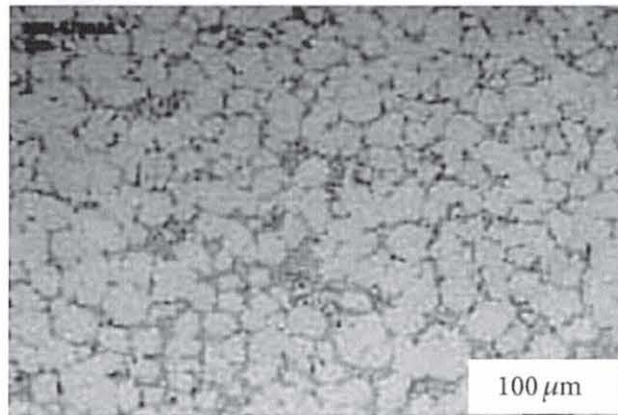
Figure 2. 8: Microstructure of 356 alloy produced by the
SSR process (Yurko et al., 2003).

2.3.8 Direct Thermal Method

In 2002, University College Dublin established the Direct Thermal Method (DTM)
of rheo-casting as an alternate material intended for producing thixotropic feedstock (M. J.
Hussey, 2002). Pouring LSH matrix into such a thin-walled mould with great conduction
properties and low thermal mass is the method used in this process. The heat is rapidly
absorbed by the melt at the initial contact of the liquid metal with the mould wall, resulting
in different nucleation. As an outcome of these scenarios, the molten alloy cools extremely
slowly and at a very low rate, starting to lose heat to the atmosphere in order to achieve an
equilibrium temperature below the alloy's liquidus (solidification range). The heat match
between the mould and the alloy causes a pseudo isothermal holding state, resulting in low
heat convection transition and a low heat gradient (D. J. Browne et al., 2003). The mould
and its contents are quickly quenched in water according to the preferred microstructure and
the predetermined temperature. Essentially, the mechanism of dendrite disintegration for this
procedure is one that generates several locations of nucleation at the start of the process,
resulting in a slower cooling to slow the possibility of dendritic arms without the use of any
special heating equipment or specific insulation (M. J. Hussey, 2002), as shown in
Figure 2.9. The microstructure of A356 aluminium achieved by the DTM is shown in
Figure 2.10. This method is regarded as the most cost-effective, and it is suitable for
laboratory activities that need only a limited number of billet sizes (M. J. Hussey, 2002).

18
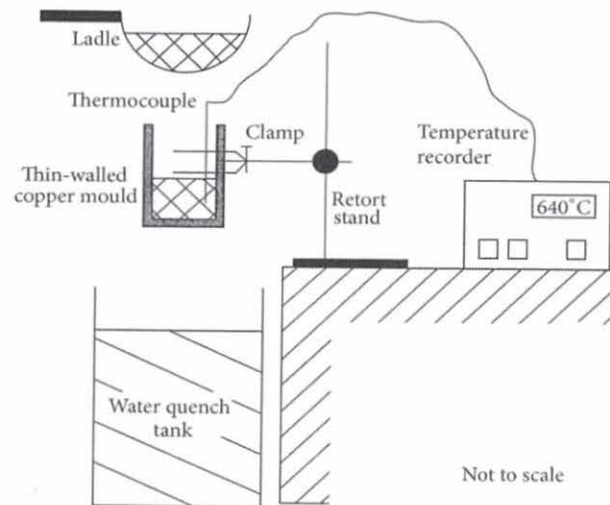
Figure 2. 9: Illustration of experimental procedure of the DTM (Browne et al., 2003).
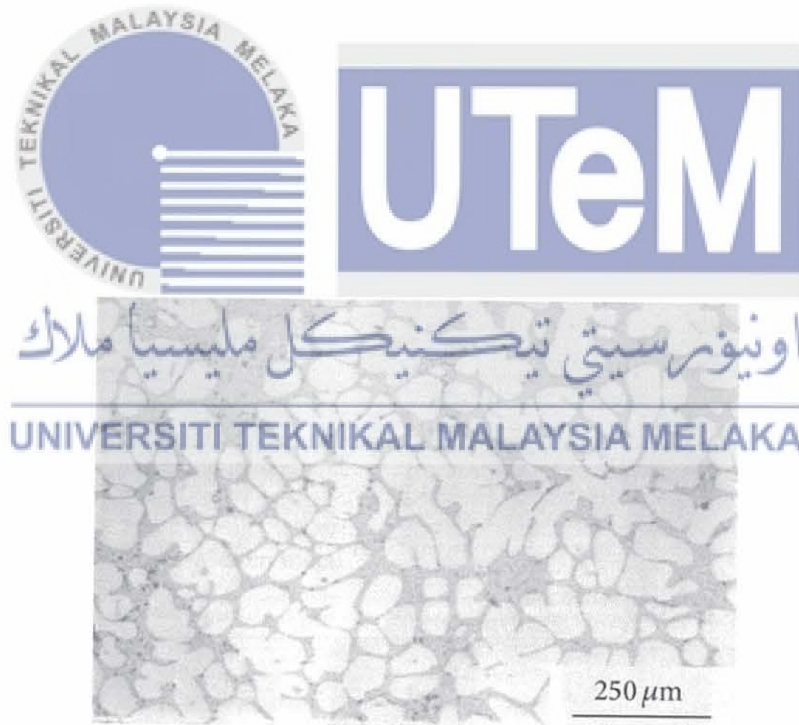
Figure 2. 10: Microstructure of alloy A356 obtained by the DTM (Browne et al., 2003)

2.3.9 Gas-Induced Semisolid Process

A novel approach to microstructure refinement that uses small gas bubbles inserted during solidification to stir up the melt as it cools to a semi-solid range to achieve a non-dendritic appearance. In the gas-induced semi-solid (GISS) process, fine gas bubbles can be incorporated into molten metal in various configurations (J. Wannasin et al., 2006; J. Wannasin and S. Thanabumrungkul, 2008). After the diffuser is removed, the semi-solid metal slurry is either injected directly into the casting device or slowly cooled until the desired microstructure and solid fraction are accomplished, as shown in Figure 2.11 and Figure 2.12. This technique's mechanism of dendrite fragmentation can be expressed as follows: The low superheat temperature allows a large number of small dendritic grains to precipitate and form on the top surface of the cold graphite diffuser when it is immersed in the melt. The movement of gas bubbles allows these particles to be quickly extracted into the melt. The fine grains were re-melted as a result of the surrounding bulk liquid, which still contained small areas of superheated liquid. Only a small number of particles remain in the molten metal. These particles are also developed by removing heat from the melt for a predetermined amount of time, resulting in fine, non-dendritic microstructures (J. Wannasin et al., 2010). The GISS method is appropriate for processing various alloys such as zinc alloys, cast aluminium alloys, wrought aluminium alloys, and die casting aluminium alloys (J. Wannasin et al., 2010).

Figure 2. 11: Schematic diagram of the steps of the GISS method (Wannasin et al., 2010)
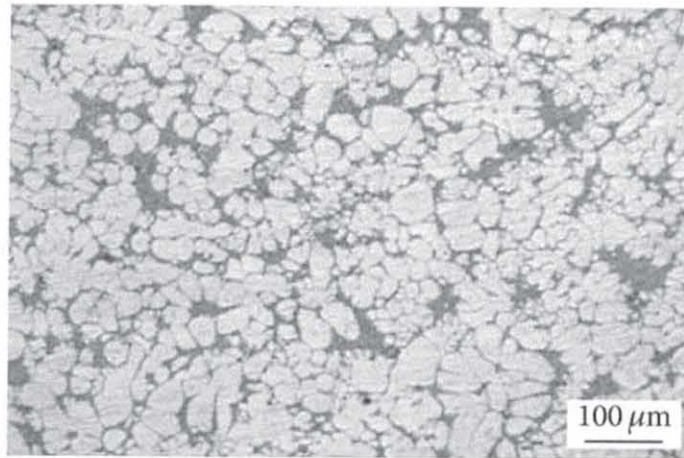
Figure 2. 12: Morphology structure of 356 aluminium alloy
gained by the GISS Method (Wannasin et al., 2010).

UTeM

اونيۏرسيتي تيكنيكل مليسيا ملاك

UNIVERSITI TEKNIKAL MALAYSIA MELAKA

2.3.10 Ultrasonic Vibrations

Ultrasonic vibrations, which were patented in the mid-1970s, are another option method for preparing feedstock for semi-solid forming processes. It works by injecting high-power ultrasonic vibrations (high frequency mechanical waves) into a cooling melt in order to maximize the amount of solidification nuclei. The practice of pulsed ultrasonic vibrations in the melt throughout solidification promotes cavitation, which causes huge immediate fluctuations in the pressure and temperature of the melt, resulting in homogenous, globular microstructures (V. Abramov et al., 1998) (Figure 2.13). Figure 2.14 depicts the microstructure of A390 aluminium generated by implementing this method. This technique's mechanism of dendrite fragmentation is characterized by two basic physical phenomena: cavitation and acoustic streaming. Cavitation is the formation, growth, pulsation, and collapse of tiny bubbles in molten metal. The compression rate of these unstable states can be so high that their destruction generates hydraulic shock waves, which disintegrate the primary particles and generate artificial sources of nuclei. The propagation of high-intensity ultrasonic waves in the melt also includes the commencement of steady-state acoustic streaming. The combined impact of these various streams is to actively mix and thus homogenise the melt (V. Abramov et al., 1998).
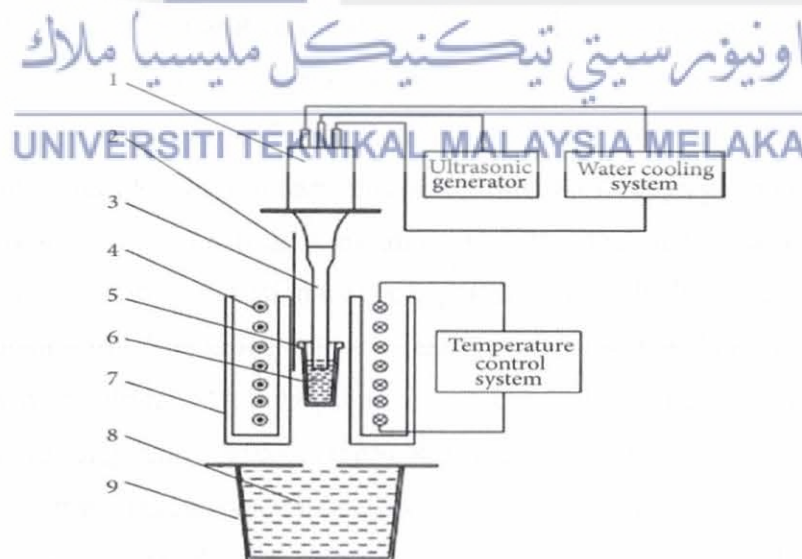
Figure 2. 13: Schematic diagrams of the ultrasonic vibration device: (1) ultrasonic transducer; (2) thermocouple; (3) ultrasonic radiator; (4) resistance heater; (5) iron crucible; (6) Mg-9.0Al%; (7) ceramic tube; (8)water; (9) tank (Zhang et al., 2008).

22
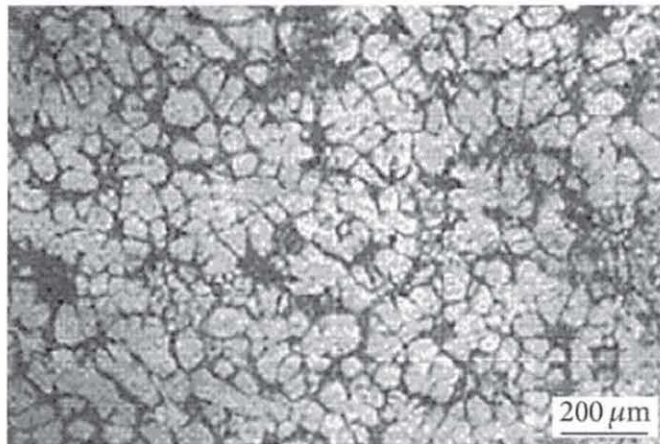
Figure 2. 14: Morphology structure of 390 aluminium alloy
obtained by Ultrasonic Vibration (Luo et al., 2010).

2.3.11 Shearing-Cooling Roll

The Shearing-Cooling Roll (SCR) process is a liquid-state process that has been developed as an alternative technique for the production of thixotropic feedstock with commercial potential. Figure 2-15 depicts the working principles of the SCR process for preparing semi-solid alloy. In summary, this method involves applying superheat to the alloy melt at a constant temperature near or just above liquidus. The molten metal is poured into the inlet of a rotating roll and a stationary cooling shoe cavity, which creates frictional forces due to the rotating roll. The molten alloy is steadily cooled by the shoe and the roll in the roll-shoe cavity, resulting in globular, semi-solid slurries due to the shear forces produced (M. Kiuchi and S. Sugiyama, 1995). In the SCR process, the formation and evolution of non-dendritic microstructures can be explained as follows. The nucleation of granular dendritic crystals occurs when the molten alloy cools at the contact surface of the roll-shoe. These are crushed and dispersed into the melt by the shearing force and stirring of the roll during solidification of the liquid alloy with high solid fraction to form equiaxed or spheroidal grains. The use of high solidification rates combined with high shearing rates in the SCR process can result in fine and well-spheroid particles in the liquid matrix (S. Wang et al.,

23

2006). The microstructure of A2017 aluminium produced by the SCR method is shown in Figure 2.16.
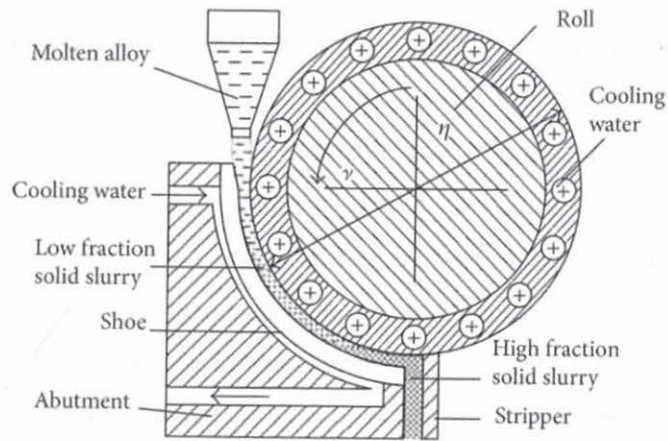
Figure 2. 15: Schematic diagram of SCR process (Wang et al., 2006).
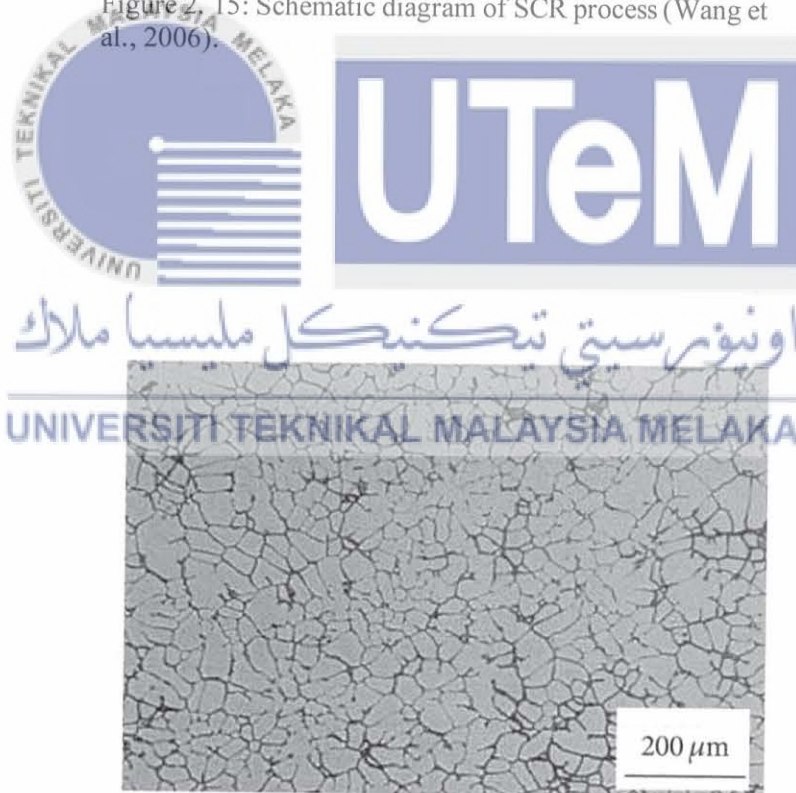
Figure 2. 16: Microstructure of A2017 aluminium alloy obtained by SCR Process (Wang et al., 2006).

2.3.12 Stress-Induced and Melt-Activated Process

One of the most successful and commercially accessible solid-state processes is the Stress-Induced and Melt-Activated (SIMA) process. In a nutshell, this technique involves reheating distorted material into a semi-solid state. The initial deformation appears above the temperature of recrystallization (hot working). Afterward there's cold working at room temperature, which is a crucial phase in loading energy flow as a result of partial re-melting, in which the material reaches a semi-solid state and uniform, non-dendritic, globular solid particles are obtained within a liquid alloy, as shown in Figure 2.18. During partial re-melting of the distorted material to recrystallize as well as create fine, non-dendritic microstructures by a mechanism of liquid absorption of high-angle grain boundaries, the morphology structure evolves into a spheroidal morphology structure. When recrystallization occurs, liquid metal with high-energy infiltration flows through high-angle grain boundaries, evolving globular solid particles in a liquid matrix. The rate of heating and the degree of cold work are directly proportional to the size of the globular solid particles. The resulting particles can be as small as 30 μm. (Young et al., 1982; Kamran 2009). The microstructure of A7075 aluminium generated by applying the SIMA process is shown in Figure 2.18.
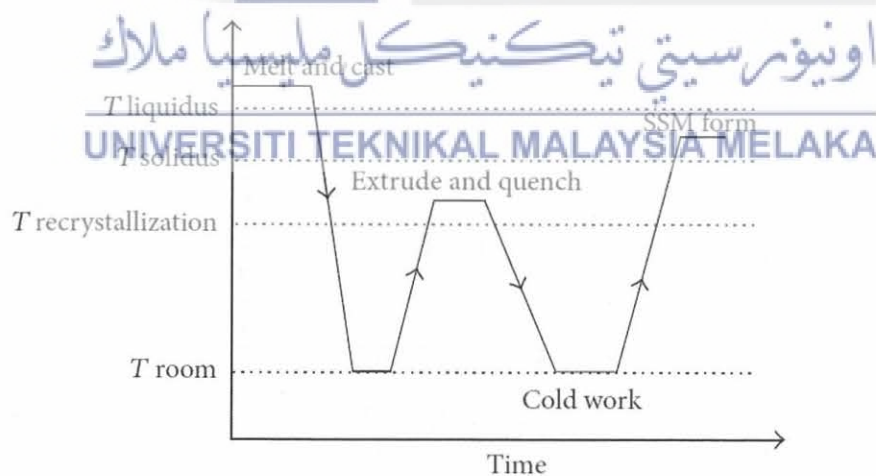
Figure 2. 17: Schematic illustration of the stages of the SIMA process (Young et al., 1982).
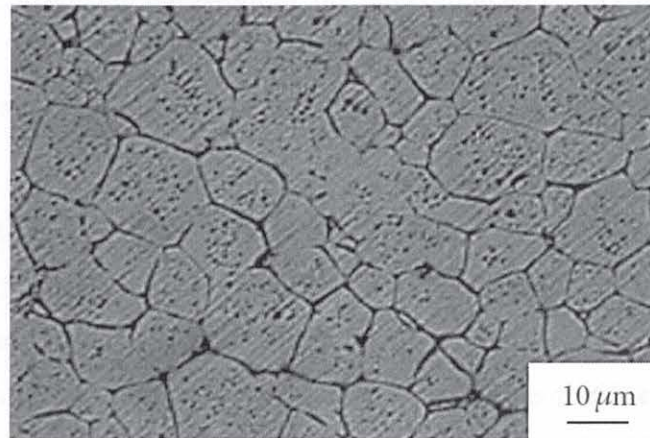
Figure 2. 18: SIMA deformed microstructure of Al 7075 alloy achieved in the case of isothermal holding at 620C for 5min (Mohammed et al., 2012).

2.4 Stir Casting
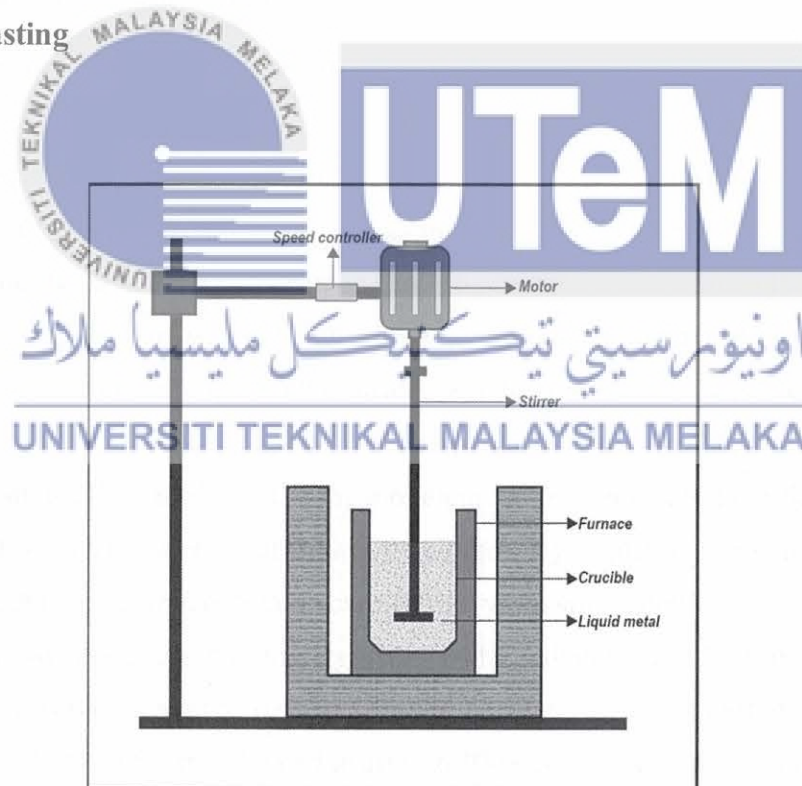
Figure 2. 19: Schematic Diagram of Stir Casting (Prabu et al., 2006)

At a constant stirring temperature, the interaction between stirring time and speed stir cast relied on. The strength of the mixture developed as the stirring time and speed were elevated at the same time Figure 2.19 above shows the schematic diagram of stir casting process.

Based on Jameel et al., (2013) the electric mixer is placed in the crucible furnace, which is spun at a high speed of 900 rpm for 3- 5 minutes to promote homogenization of the molten material, and then the molten material is poured into a pre-heated metallic mould. The authors concluded that increasing the amount of reinforcement in composites up to 20% increased the hardness, ultimate tensile strength, and yield strength of the material. With the addition of reinforcement, the impact energy was reduced. The microstructural analysis revealed a consistent distribution of particles. The insertion of reinforcement wrapped in aluminium foils, as well as the injection of magnesium to the molten metal, were the specific causes of this (Jameel et al., 2013).

To stir molten metal and produce the vortex, S. Balasivanandha Prabu et al. employed a mild steel impeller spinning at 500–700 rpm (Because of the centrifugal forces generated by the vortex, the secondary phase is thrown against the crucible walls, guaranteeing uniform distribution of particles in the matrix). To achieve particle mixing, the impeller blades were intended to create vortex. To prevent blade dissolving in molten metal, a zirconium-based coating was put to the impeller (additionally to avoid metal pick-up also to avoid molten metal reacting with the stirrer). A mechanical stirrer was used to agitate the molten metal and induce turbulence during the operation. Immersed impeller was at a depth of approximately 2/3 of the height of the molten metal from the bottom of the crucible and the speed of the stirrer was set at 500/600/700 rpm. By adjusting the stirring speed and stirring time, the molten metal–Silicon carbide slurry was stirred continuously for the various combinations of processing parameters. After adding Silicon carbide to the solution, the stirring time was recorded at 5, 10, and 15 minutes. The molten aluminium was put into a mild steel die that had been preheated to around 300 degrees Celsius. They discovered that when stirring speed and time were reduced, clustering occurred, and some areas were identified without particle entrapment, but that when stirring time and speed were increased, the dispersion became more homogenous. The composite's hardness increased as the stirring speed and time increased (Prabu et al., 2006).

2.5 Thixoforming Process

The globular morphology, rather than the dendritic microstructure, is the important ingredient in the SSMP, and it is the thixotropic nature of the semi-solid slurry that lowers segregation and porosity inside the castings. SSMP has various benefits over previous procedures, including improved product quality, reduced forming temperature, greater production rate, and improved mechanical qualities through microstructural refinement. Other than the rheocasting technique SSMP techniques based on the thixotropic characteristic of alloys with non-dendritic composition in the semi-solid state include thixoforming. Thixoforming and associated SSMP processes, require thixotropic feedstock materials as a compound. The figure 2.20 below shows Schematic illustration of (a) Rheocasting process (b) Thixoforming process (Song et al., 2020).
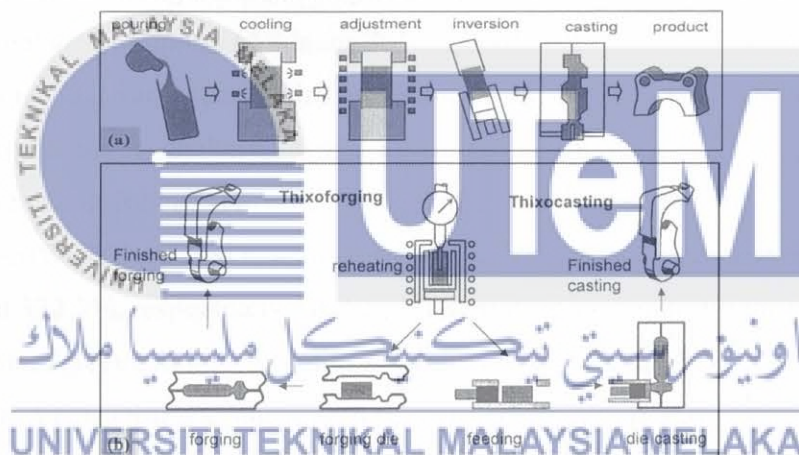
Figure 2. 20: The figure shows Schematic illustration of
(a) Rheocasting process (b) Thixoforming processes
(Song et al., 2020)

2.5.1 Shear Mechanism in Alloy

An alloy where, in this case, when the material state is 50% solid and is sheared, the coalescence of the material will break up, its viscosity will fall, and it will flow like a liquid, but if it is allowed to stand for a certain time, globular coalescence will increase the viscosity of the material, which leads to it being able to support its own weight and be handled in the same way as if it was solid. As described above, a globular microstructure with an appropriate amount of liquid fraction is required in order for the SSM forming to be

28

successful. When shear forces are applied, the near-globular particles move easily past one another, causing a decrease in viscosity and making the material behave like a liquid. In contrast, when shear forces are applied on dendrite microstructures, typical of conventional castings, the liquid is trapped between dendrite arms and prevents them from moving freely, thus increasing the viscosity of the material (Mohammed et al., 2013).

2.5.2 Thixoforming towards Mechanical Strength Al-Matrix

In comparison to the non-thixoformed composite samples, the Yield Strength (YS), Ultimate Tensile Strength (UTS), and elongation to fracture of the samples after thixoforming increased by 33.3 % (180.0 MPa), 43.3 % (255.8 MPa), and 83.9 % (5.7%) respectively. Thixoforming is a well-established method for reducing or eliminating porosity. Hence, the strength and ductility of thixoformed samples should be improved if the porosity is kept to a minimum (Atkinson & Liu, 2010; Peng et al., 2011). Furthermore, it is widely assumed that during partial thixoforming, the homogenous distribution of MWCNT in the matrix remains unaltered while concurrently filling the pores, improving the microstructure's compactness (Li et al., 2016). Mechanical stirring, thixoforming, and a brief T6 of A356-MWCNT resulted in an increase in mechanical characteristics of up to 87.0 %, 108.4%, and 322.2%, respectively, for YS, UTS, and elongation to fracture. These results showed a good agreement with Elshalakany et al. (Bakr et al., 2014), who also found that the maximum YS, UTS and elongation to fracture of 1.5 wt% of MWCNT A356 composite fabricated using rheocasting or squeeze casting were improved by 60%, 50% and 320%, respectively. The composite strength produced in these investigations was within the required range of 250-300 MPa for automotive parts according to Tavitas- Medrano et al. (Tavitas-Medrano et al., 2008).

2.6 T6 Heat Treatment

2.6.1 T6 Heat Treatment Towards Microstructure Al-Matrix and Mechanical Strength Analysis

Heat treatment involves a number of simple steps in producing desired mechanical properties in a controlled way to exploit the outstanding behaviours of metal, such as making them stronger, increasing malleability, increasing ductility and increasing resistance to abrasion.

Heat treatment helps modify alloys' microstructures without compromising their ability and their structure of the entity that involves solution treatment, quenching and artificial aging, as many past studies have proved that right after five minutes of the solution of heat treatment, silicon particles in aluminium Al 319 start to develop and change into more globular microstructures (Rahman et al., 2020). However, in 2001 and 2016, researchers such as Jerry et al., and Costa et al., proposed a methodology that involved four steps to perform T6 heat treatment with expected time and controlled temperature (Table 2.8). This research is then continued by Magno et al., 2017 stated that the aimed of solution treatment is to dissolve $Al2Cu$ which is in intermetallic states in Al- rich matrix (α-Al)and get the equilibrium state, while in quenching step the formation of $Al2Cu$ intermetallic metastable phase can eventually spread in α-Al solution by the help of warm water to produce superheated solid solution that will precipitated lastly in aging step (Figure2.9) (Magno et al., 2017). Conventional T6 heat treatment will take a longer time to complete the whole processes (three main processes), according to Hashim et al., 2021, as the minimum duration of 9 hours needed to complete the processes, solution treatment at 50°C required 6 − 12 hours and for artificial aging another 3 to 5 hours will be spend to complete the process at 155°C (Hashim et al., 2021).

Process / Stages	Expected Time, Hours	Controlled Temperatures, in °C
Solution Heat Treatment	5 h	490°C ±2°C
Quenching in warm water		60°C ±2°C
Immediate Aging	3 h	155°C ±2°C
Air Cooling		

Table 2. 8: Methodology Proposed by Jerry et al.,2001 and Costa et al., 2016

TEMPERATURE (°C)

SOLUTION HEAT TREATMENT (490 °C)

QUENCHING (60 °C)

AGING (155 °C)

TIME (h)

5 h   3 h
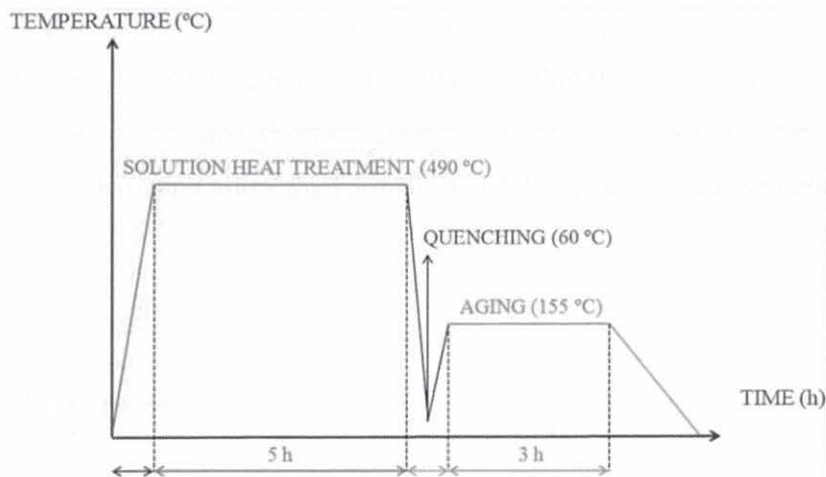
Figure 2. 21: Stages of T6 heat treatment applied represented schematically (Magno et al., 2017)

2.6.2 Short Heat Treatment

A new T6 heat treatment with solution times less than 30 minutes showed better properties in mechanical properties compared to old and standard conditions of heat treatment that needed a minimum of 9 hours to complete 3 stages involved in producing SSM composites. According to previous research, researchers stated that the time of 50 mins with 540°C in solution treatment is sufficient enough to produce α – aluminium dendritic microstructure with homogeneous distributed silicon and Mg while only 30 minutes is needed for solution treatment when casting A356 alloy at 540°C for low pressure die casting. Thixoformed samples will be treated with shorter solution treatment at 540°C for 1 hour, followed by quenching in water at 26°C and 27°C, room temperature before being aging artificially for 2 hours at 180°C using Nabertherm 30°C to 30000 °C furnace (as shown in Figure 2.10) in short T6 heat treatments (Hanizam et al., 2019). Significantly, reducing solution treatment time when applied in SSM has big impacts on productivity because the cooling rate is faster compared to HPDC, High Pressure Die Casting generating inter-metallic compounds with more small in size and more homogeneous structured components that are near to eutectic microconstituent in α – phase globules as well as the economic issues (Menarguesr et al., 2015).

Whereas, Chinese researchers showed in graphical approaches that UTS and elongation percentage of Al - composite alloy were improved 31% and 23 % respectively

31

compared to as-cast alloy and nearly same mechanical properties to conventional T6 heat treatments (Lu et al., 2018). Chen et al., 2018 said that their results revealed a new heat treatment method, or that this short heat treatment process is able to minimize the growth rate of eutectic silicon and allow the formation of fully spheroidization of eutectic silicon.
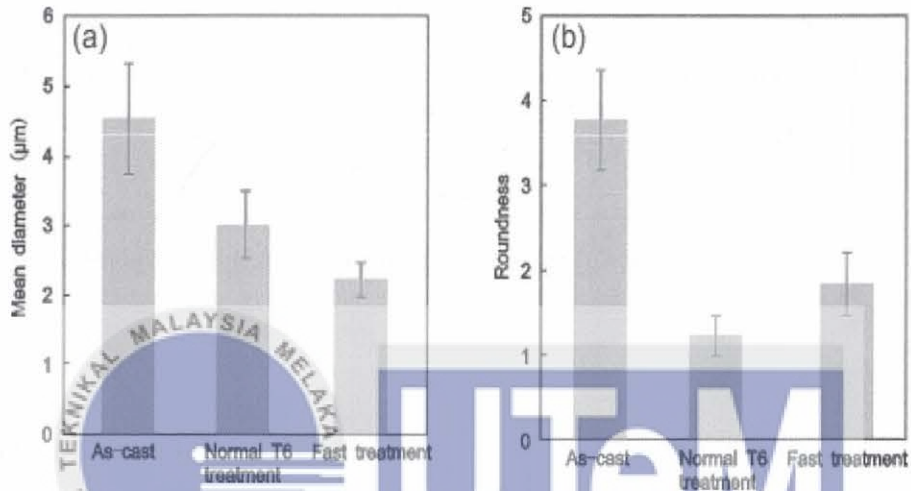
Figure 2. 22: Comparison of average values of (a) mean diameters and (b) roughness for As-cast and T6 Treatments (Lu et al., 2018).
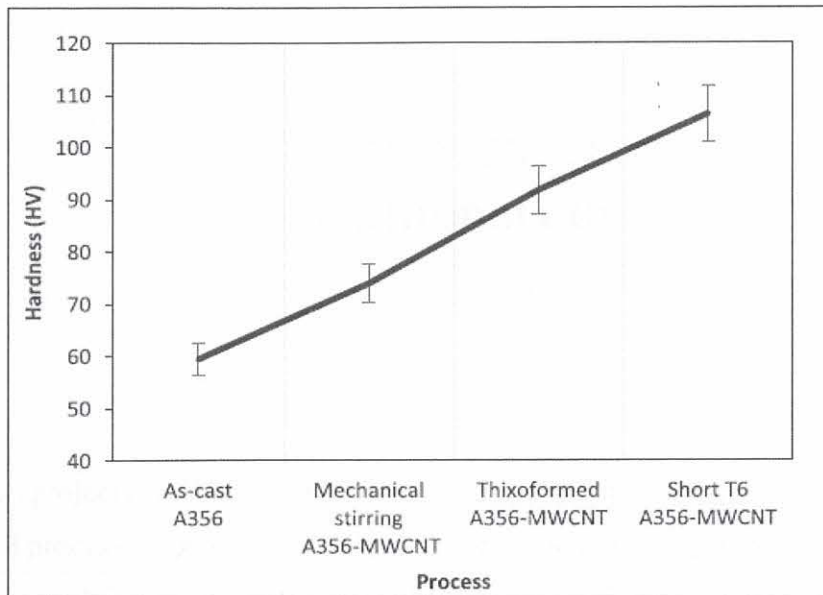
Figure 2. 23:Hardness values of each stage (Choi et al., 2011)

The hardness of the studied samples is shown in Figure 2.23. Compared to the as-cast A356 alloy (59.5 HV), the hardness of A356-MWCNT composite (73.9 HV) increased by 24%, demonstrating the direct influence of MWCNT in the matrix. After being treated to thixoforming and brief T6 heat treatment operations, the hardness of the composites increased to 91.8 and 106.4 HV, respectively. The uniform distribution of MWCNT in the matrix is responsible for the increase in hardness, porosity decrease, and reduction of microstructure grain size. In the previous section, the impacts of dispersion and porosity filling were discussed. Thus, grain refinement could be predicted based on Hall-Petch strengthening mechanism (Choi et al., 2011). The grain size, on the other hand, only accounted for roughly 70% to 80% of the reinforcing strengthening process (Bradbury et al., 2014). The hardness of crystallites decreases as the crystallite size decreases, according to the Hall-Petch strengthening principle (Bradbury et al., 2014). As a result, it is proposed in this study that the composite's high hardness was caused by two actions: first, mechanical stirring, which contributed in smaller and more uniform dendritic structure fragmentation; and second, the addition of MWCNT, which acts as heterogeneous nucleation, encouraging even more grain refinement to the grain sizes (Bakr et al., 2014).

33

CHAPTER 3.0
METHODOLOGY

This project is to determine and describe the analysis of different processes of semi-solid metal processing that will be affecting the aluminium alloy LM21/A308 feedstock. This project established quantitative data of analytical mechanical properties and qualitative data of microstructural aluminium alloy when experienced mechanical stirring casting for the preparation of thixoforming process. The data that is to be collected is solely from my experiment. From this experiment, the experimental data that will be gathered are observations without intervening by controlling any parameters. However, manipulating variables were the processes that were chosen as to stir casting, thixoforming and T6 heat treatment process.
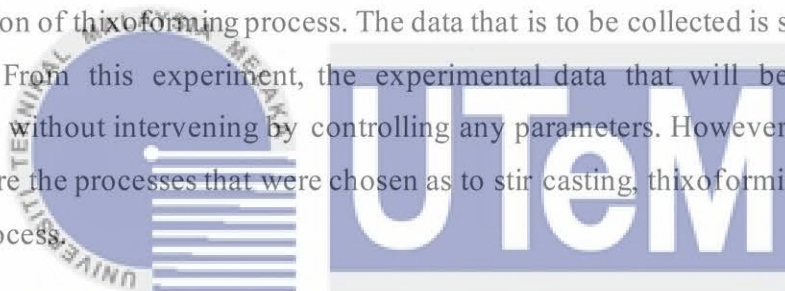
The relationship between the objective and methodology is as shown below in Table 3.1.

Table 3. 1 :Relation between Objectives with Methodology of Project

OBJECTIVE	METHOD
1) To produce aluminium alloy for thixoforming using partial remelting.	Preparing LM21/A308 for billet feedstocks • Stir casting Partial Remelting Process/ Secondary process • Thixoforming process Heat treatment • T6 Heat treatment
2) To investigate the microstructural evolution of aluminium alloy after partial remelting.	Characterization of Morphology and Microstructure Material • SEM
3) To determine the mechanical properties of thixoformed aluminium alloy	Mechanical test • Tensile test • Vickers Hardness Test

34

Below is the Flowchart presented to follow the methodology in Figure 3.1.
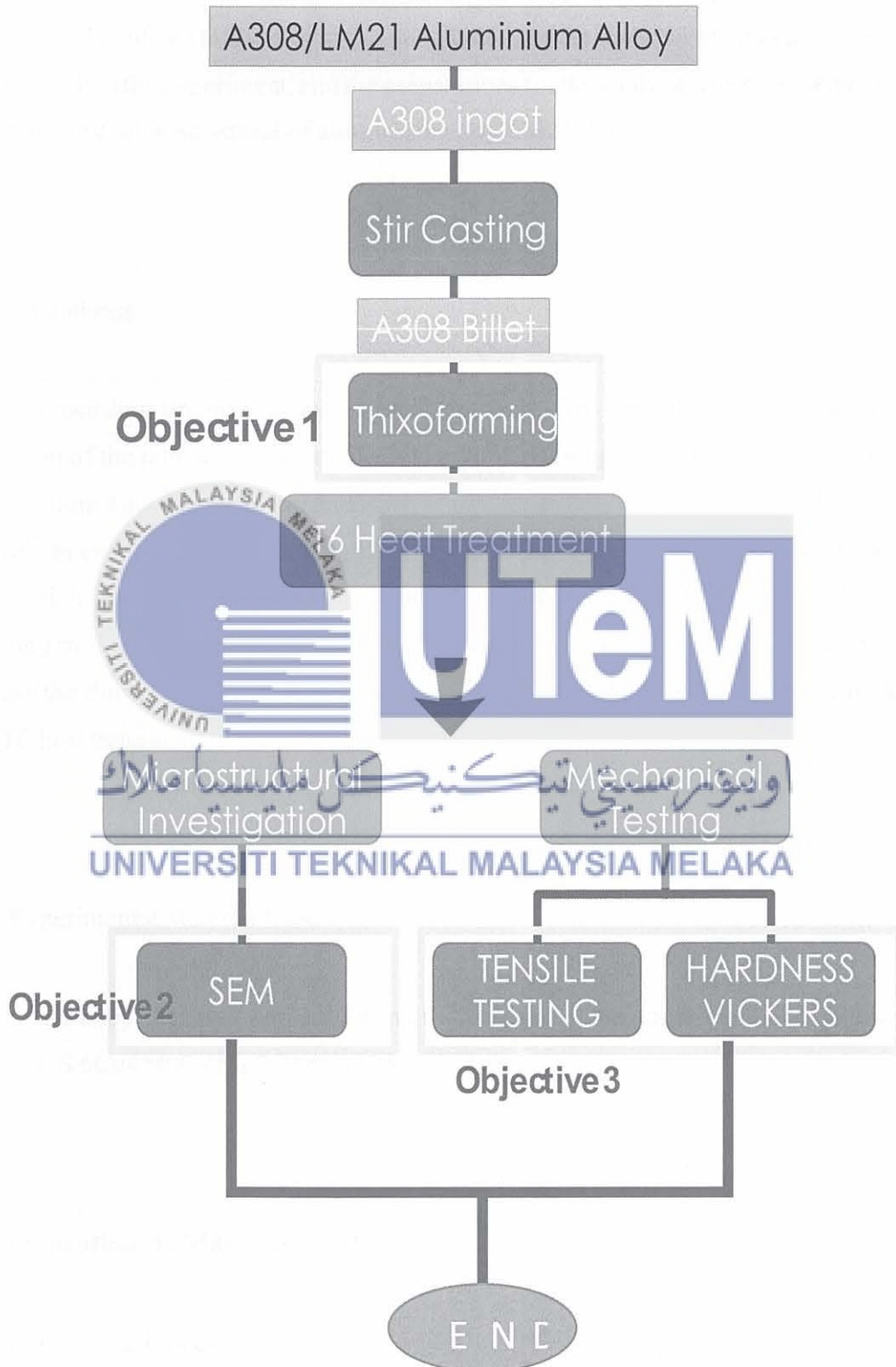
Figure 3. 1 :Flowchart of Methodology Process

3.1 Experimental Design

My experimental design included the hypothesis, experimental material, experimental methods that will be explaining details of the tools, techniques and procedures used to conduct the experiment, and the preparations for the analytical testing for mechanical properties and microstructural of aluminium alloy LM21/A308.

3.1.1 Hypothesis

Depending on my discipline and approach, this methodology begins with the discussion of the rationale of my methodology underpinning to semi-solid metal processing of aluminium alloy. By using stir casting, it can produce a globular, spheroidal and non-dendritic microstructure for aluminium alloy feedstock. Otherwise, the end result alloy will have a high porosity that will lead to an easily broken product. Moreover, the partial remelting process will avoid the creation of a dendritic microstructure in the join zone and increase the ductility of the material. To increase the strength of the material, it is treated with T6 heat treatment.

3.1.2 Experimental Material Used

The alloy that was applied during the process was commercial LM21 aluminium alloy (Al-Si6Cu4Mn0.4Mg0.2) or A308.

3.2 Preparation of Material Used

3.2.1 Stir Casting Process

All metal used in this experiment was weighed accurately for 400g. No recycled aluminium was used for any of the tests. Materials were charged into a steel crucible, and the crucible

was loaded into a resistance pit furnace in a lift coil type induction melting furnace. A proprietary gas cover of SF6 +CO2 was provided on the melted surface continuously to prevent oxidation and burning of the material. The temperature of the melt was monitored from time to time with the digital temperature detector. In the case of this aluminium alloy, the furnace temperature was set at 700^0C and the furnace was loaded with a crucible containing the required amount of Al. The required amount of Al (400g) was added to it after melting of Al and charge was held for about 45 minutes to an hour. After it reached the desired temperature, the mechanical stirrer was used by using the impeller for 5 minutes at 500rpm. The metal is awaited to a temperature of 700^0C then directly poured into the mould. The entire procedure was carried out in a moisture-free environment with safety guarded with masks, gloves, safety shoes and protective goggles.
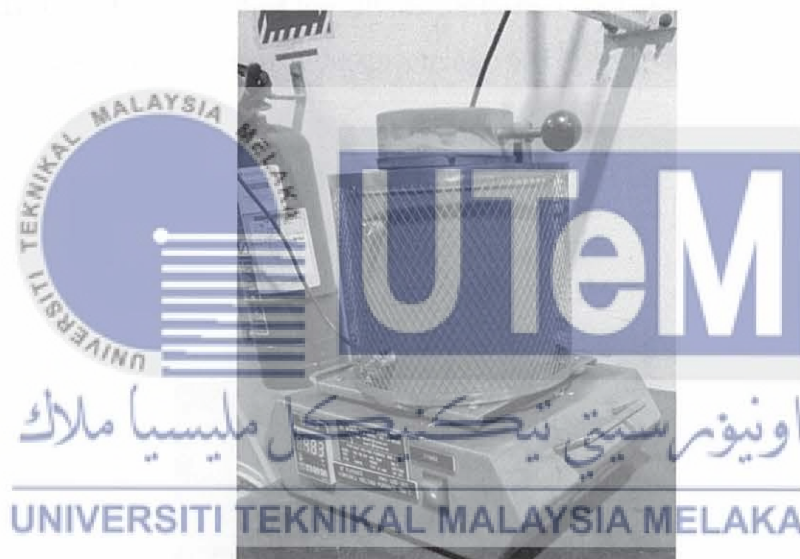
Figure 3. 2 :Stir Casting Process (Kumar et al., 2014).

3.3 Processing

3.3.1 Thixoforming Process

After the stir casting process, 8 billets were taken to be used for the thixoforming process. The T30-80 KHz thixoforming machine was used for the thixoforming process (Fig. 3.3).

For the thixoforming process, the measurement needed for the billet was 11cm to fit the place in the coil induction and the temperature of compress was 502 ^{0}C. The thixotropic billet was reheated to a semi-solid temperature of 510 ^{0}C using a pneumatically operated ram inside an induction coil, yielding a liquid fraction of 50 percent. The reheating operation was managed by gradually increasing the heating frequency at a rate of 10 A per minute until the temperature was reached. The billet was then rammed into a preheated (100^{0}C) hot work tool steel mould on top of the coil with a forging weight of 5 tonnes at a speed of 1 m/s. After that, the billet was removed from the mould and allowed to cool to ambient temperature (Hanizam et al., 2019). The specimen was removed from the compressed mould and cooled at room temperature after holding. During this process, the situation of elephant foot happening to the specimen must be avoided. When finished, by reaching 8 billets of thixoformed process, the samples are divided into two so there will be 4 samples for thixoformed and 4 more samples for the upcoming T6 HT process.

Figure 3. 3: Thixoforming T30 Machine

Figure 3. 4: Induction coil in Thixoforming Machine
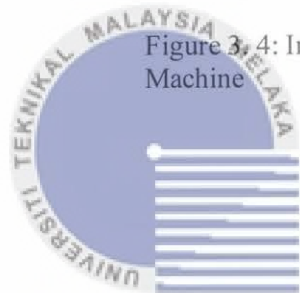
3.3.4 Heat treatment

The heat treatment was only for the thixoformed parts of sample. For the aluminium alloys, the T6 heat treatment cycle was designed by first plotting the ageing curve to determine the peak ageing time. For this, the samples were solutionized for 8 hours at $540^{0}C$ and quenched in ambient water at room temperature then aged for 4 hours at $180^{0}C$.
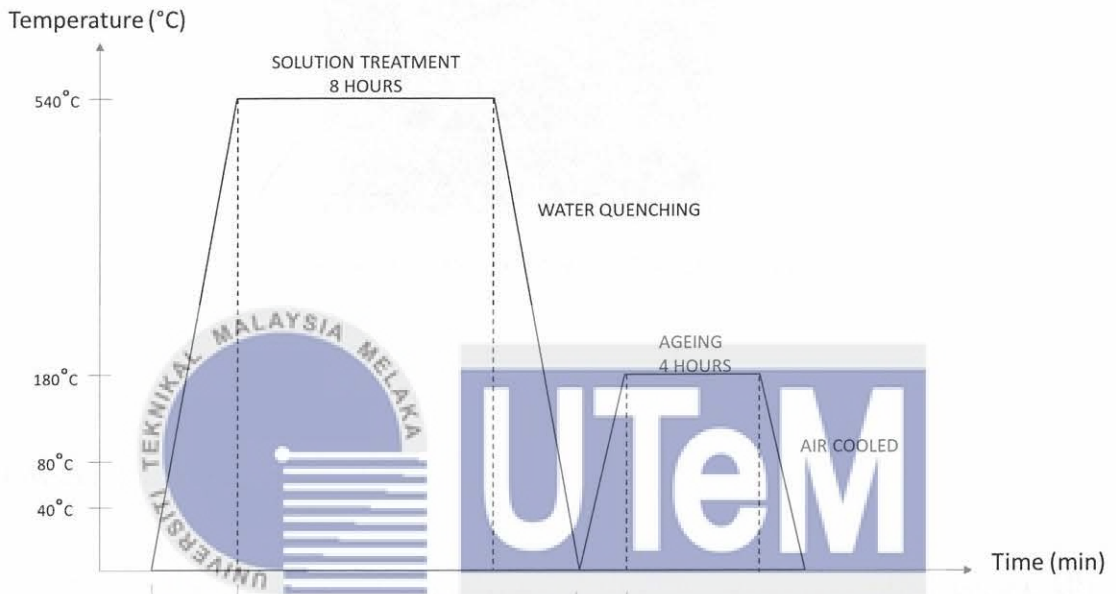
Figure 3. 5: Schematic Diagram of Solution Treatment and Ageing Graph
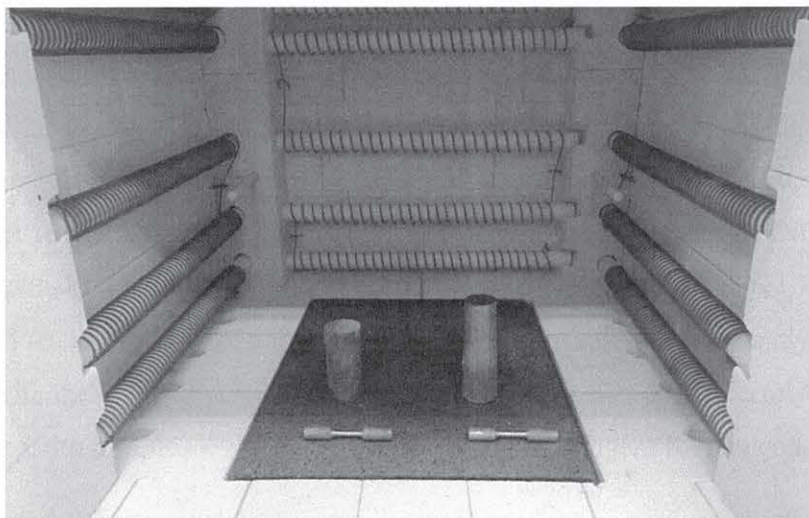
Figure 3. 6: Samples for Microstructural and Mechanical Testings in Furnace

Figure 3. 7: Furnace for T6 Heat Treatment

3.4 Microstructure Analysis

The as-cast, thixoformed and thixoformed T6 samples were verified using CARL ZEISS EVO 50 scanning electron microscope (SEM). This machine will aid in the investigation of the morphology and composition of the LM21/A308, which was used for microstructure observations.

Before undergoing the Scanning Electron Microscope (SEM), samples of the as-cast, thixoformed and thixoformed T6 were first being grinded with NANO2000T Grinder. The rough grinding with PACE SIC grinding paper that were used are 240, 320, 400, 600 grit at 150-200 rpm. The fine grinding with PACE SIC grinding paper that was used was 800 and 1200 grits at 150-200 rpm. The samples were then polished using the NANO200T polisher. The rough polishing that was used was 1 micron at 150 rpm with PACE TEXPAN polishing cloth and PACE DIAMAT polycrystalline diamond suspension. Lastly, use the fine polishing with the PACE NANOPOLISH alumina suspension 0.05 micron. Once done with the polishing, the samples were then etched in Keller's Reagent for 5 seconds.

41
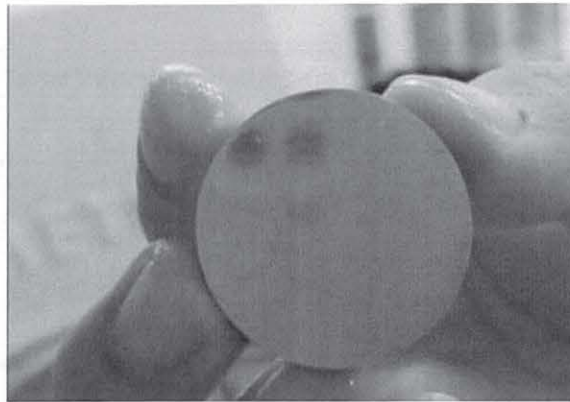
Figure 3. 8: As-cast sample after grinded and polished before etching.

3.5 Mechanical Testing

3.5.1 Tensile Test

All tensile tests were carried out in accordance with ASTM E8M, with dimensions comparable to standard in the small-size specimens. The small-size specimens were used because in many cases the area to be tested was just too small to cut a full-size tensile specimen. The CNC Turning machine was used to prepare the sample and ensure that the tensile test samples were perfectly measured.
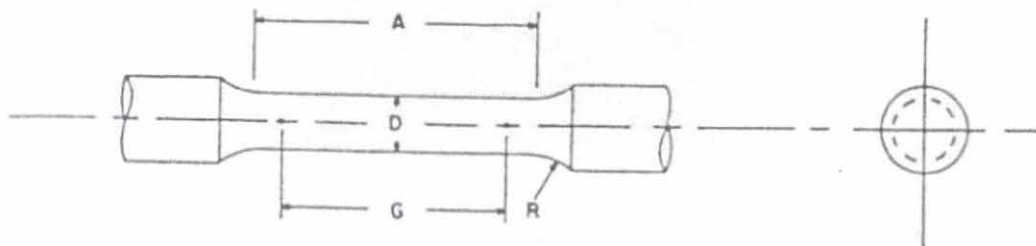
Figure 3. 9: ATSM E8 Tensile bar schematic (Zhu et al., 2013).

Table 3. 2: ASTM E8 Tensile bar dimensions (Zhu et al., 2013).

| | Dimensions, mm [in.] For Test Specimens with Gauge Length Five times the Diameter [E8M] | | | | |
| | Standard Specimen | Small-Size Specimens Proportional to Standard | | | |
	Specimen 1	Specimen 2	Specimen 3	Specimen 4	Specimen 5
G—Gauge length	62.5 ± 0.1	45.0 ± 0.1	30.0 ± 0.1	20.0 ± 0.1	12.5 ± 0.1
	[2.500 ± 0.005]	[1.750 ± 0.005]	[1.250 ± 0.005]	[0.800 ± 0.005]	[0.565 ± 0.005]
D—Diameter (Note 1)	12.5 ± 0.2	9.0 ± 0.1	6.0 ± 0.1	4.0 ± 0.1	2.5 ± 0.1
	[0.500 ± 0.010]	[0.350 ± 0.007]	[0.250 ± 0.005]	[0.160 ± 0.003]	[0.113 ± 0.002]
R—Radius of fillet, min	10 [0.375]	8 [0.25]	6 [0.188]	4 [0.156]	2 [0.094]
A—Length of reduced section, min (Note 2)	75 [3.0]	54 [2.0]	36 [1.4]	24 [1.0]	20 [0.75]

3.5.2 Hardness Test

In heat-related cases, hardness tests were carried out using Vickers hardness testers and they will be measured in terms of HV. Average 9 measurement of HV value will be converted into Vickers hardness value. The load of 1kgf and load time duration of 10 seconds will be applied.
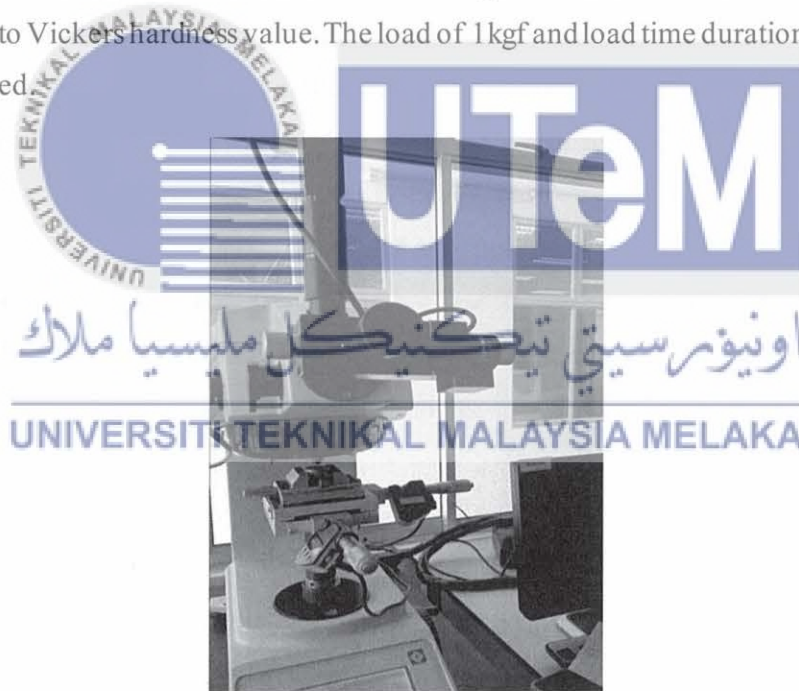
Figure 3. 10 : Vickers Hardness Tester (FKP Lab)

CHAPTER 4.0
RESULTS AND DISCUSSION

4.1 Microstructural Analysis

Before undergoing the Scanning Electron Microscope (SEM), the samples were first being grinded with NANO2000T Grinder. The rough grinding with PACE SIC grinding paper that were used are 240, 320, 400, 600 grit at 150-200 rpm. The fine grinding with PACE SIC grinding paper that was used was 800 and 1200 grits at 150-200 rpm. The samples were then polished using the NANO200T polisher. The rough polishing that was used was 1 micron at 150 rpm with PACE TEXPAN polishing cloth and PACE DIAMAT polycrystalline diamond suspension. Lastly, use the fine polishing with the PACE NANOPOLISH alumina suspension 0.05 micron. Once done with the polishing, the samples were then etched in Keller's Reagent for 5 seconds.

Figure 4. 1: SEM Images on 80X and 150X magnification
on as-cast A308 aluminium alloy.

The figure above showed that the microstructure of A308 consists of majorly α-Al dendritic arms (as marked above) as well as other intermetallic compounds. This primarily dendritic morphology, a characteristic tree-like structure in A308 containing different intermetallic phases in the inter-dendritic regions, showed homogeneous structure. As can be seen the dendritic size in A308 is fine. Stirring also helped to refine the grain structure of the microstructures (Hanizam et al., 2019). The speed of 500 rpm used contributed the formation in homogenous matrix as Prabu et al., (2006) stated that higher stirring speed gave a higher hardness of the composite. In figure 4.1, the as-cast sample produced superior non-dendritic feedstock for thixoforming, so it must be able to produce homogeneity in the

45

microstructure. Dendritics are the effect of stirring time during casting as it takes a longer time than five minutes to produce more globular, as from previous research (Adediran et al., 123 C.E.). After 5 minutes of stirring, particles are combined in higher numbers as time progresses. As previously observed, churning helped spread the particles in the molten matrix and avoided density segregation, which could explain this outcome (Hanizam et al., 2019).

Figure 4. 2 :SEM Images on 80X and 150X magnification
on thixoformed A308 aluminium alloy

Negative impacts of stirring included voids and porosities, which resulted in a drop in the composite's hardness and UTS. As a result, thixoforming and heat treatment as subsequent operations were required to mitigate such effects with an agreement of Song et al., that microstructural refining of the material is used to improve mechanical qualities.

46

Figure 4.2 above shows the microstructures and describes the influence of the secondary process where near spheroidal α -aluminium phase appeared that leads thixoforming process is better than conventional forming process. Figure 4.2 depicts rosette-like and semi-globular microstructures encircled by eutectic microconstituent generated following mechanical stirring, which is appropriate for thixoforming. The grain boundaries grew larger as the temperature rose, forming continuous -phase microstructures. Eutectic silicon (Si) regions were detected after thixoforming in Figure 4.2 in agreement with previous research (Hanizam et al., 2019).

The difference in grain size between the as-cast and thixoforming in favour of the increased heating rates used in thixoforming tests are thought to be the cause for the thixoformed part. In addition, according to Mohammed et al., (2013) in thixoforming, when shear is applied the globular coalescence will increase the viscosity of the material, which leads to it being able to support its own weight and be handled in the same way as if it was solid. That affects the grain size to be bigger since the coalescence break-up. The rounding of the grain counters must have been aided by the flow of the liquid phase under forming pressures.

SEM images of as thixoformed T6 heat treated LM21/A308 material below were solutionized for 8 hours at 540°C and quenched in water for 5 minutes at room temperature then aged for 4 hours at 180°C. The eutectic phase is derived from the solidification of the "liquid" in the semi-solid slug. The eutectic silicon particles spheroidized acquiring a more rounded shape and increasing significantly their size of the α -Al grains with the agreement of Chen et al., 2018 that short heat treatment process are able to minimize the growth rate of eutectic silicon and allow formation of fully spheroidization of eutectic silicon . The short T6 heat treatment affected eutectic morphology in the Figure 4.3 below.
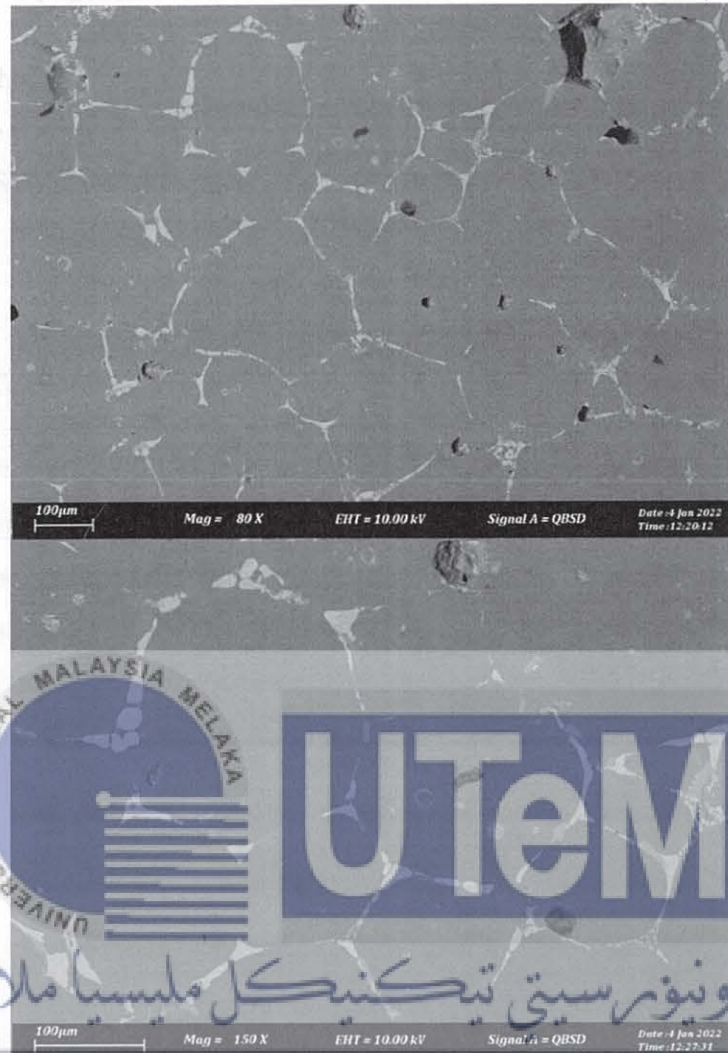
Figure 4. 3: SEM Images on 80X and 150X magnification on thixoformed T6 Heat Treated A308 aluminium alloy

4.2 Mechanical Properties Analysis

The mechanical properties that were investigated were the hardness test by using Vickers machine with ASTM-E384 Standard and tensile test by using the Universal Tensile Machine with ASTM-E8M Standard.

4.2.1 Hardness Test

To calculate the hardness test results, a sample from each process were tested using the Vickers Hardness Test machine. The data was repeated to 9 times measurement for each sample before the standard deviation value was converted into an HV unit. Table below showed hardness values for as – cast, thixoforming and thixoformed short T6 heat treatment. A sample of LM21/A308 aluminium alloy was selected for each process and the results were then presented and tabulated in a graph manner.

Table 4. 1: Hardness Test Result for as-cast, thixoformed and thixoformed T6 heat treated.

SSM Processing Type	Mechanical Properties – Hardness (HV)
As- Cast	97.5
Thixoforming	123.4
Thixoformed Short T6 Heat Treatment	128.4

Different SSM processing types will give different hardness values, the highest hardness value of these types of A308 aluminium alloy is 128.4 HV given by thixoformed Short T6 HT according to the given values. Short T6 HT attained the highest value of HV when a sample from stir-cast with thixoformed process was treated with heat treatment for 8 hours holding time at 540⁰C, quenched for 5 minutes in a room temperature water and aged for 4 hours holding time at 180⁰C plays important role to produce homogeneous sample with

49

globular microstructure. While the lowest hardness value is from as-cast which is only 97.5 HV compared to 123.4 HV and 128.4 HV for thixoforming and thixoformed Short T6 HT respectively. From the graph below (Figure 4.4), we could see the increasement of 26.56% for thixoforming sample compared with as – cast sample and about 31.69% increasement in HV for Short T6 HT compared to the as – cast, while the hardness comparison between Short T6 HT and Thixoforming samples shows only 4.05% increasement. In thixoforming sample, we could see the microstructure shows evolution from dendritic to spheroidal structure, the dendritic of the as-cast sample evolved into globular shape when thixoforming take places. The evolution showed the decreasing porosity that increase the hardness. This explained by the microstructure of each sample, Short T6 HT consists of coarser microstructure as the present of Al_2Cu particles at the end of T6 HT can dissolve eventually and diffused perfectly into the matrix region. With an agreement to Choi et al., (2011) that after being treated to thixoforming and brief T6 heat treatment operations, the composites' hardness increased to 91.8 HV and 106.4 HV, respectively. This proves that Hall-Petch theory on strengthening mechanism of the decrease of crystallite size affects the increase in hardness value (Choi et al., 2011). As a result, it is recommended that the composite's high hardness was dependent on two actions: first, mechanical stirring, which caused in smaller and more uniform fragmentation of dendritic structures, and second, the heat treatment process, which involves solution treatment, quenching, and artificial ageing and helps alter alloys' microstructures without jeopardizing their potential and structure of the entity.
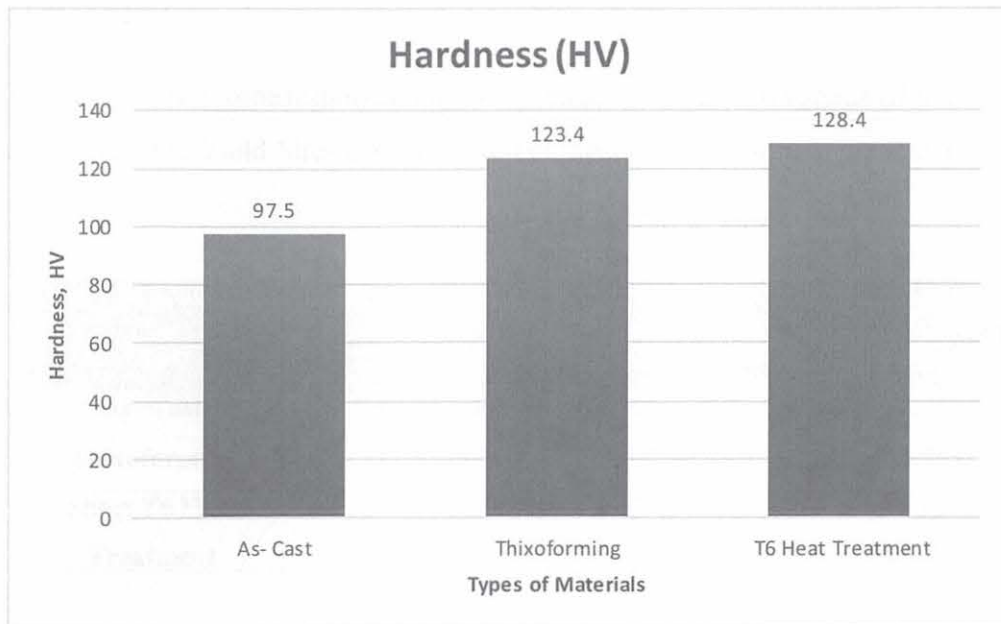
Figure 4. 4: Bar graph of Hardness Test among as-cast, thixoforming and thixoformed T6 heat treated.

4.2.2 Tensile Test

Tensile tests covered some tests to determine mechanical behaviour such as Ultimate Tensile Strength (MPa), the Yield Strength (MPa) and elongation of fracture in percentage.

Table 4. 2: Tensile Test Results

SSM Processing Type	Ultimate Tensile Test	Yield Strength	Elongation to Fracture
As- Cast	147.34 MPa	82.07 MPa	4.24%
Thixoforming	211.88 MPa	104.94 MPa	6.56%
Short T6 Heat Treatment	258.77 MPa	134.36 MPa	8.93%

Positive improvement in Ultimate Tensile Strength showed UTS graph (Figure 4.5) below from as – cast to thixoforming and thixoformed short T6 HT for A308 aluminium alloy. Same as above, each sample from each SSM process will be tested. Sample from stirred casting A308 aluminium alloy with 5 minutes stirring time at 500 rpm stir rate undergone thixoforming process then T6 heat treatment. Thixoformed Short T6 Heat Treatment sample shows outstanding tensile test results as compared to As-cast and Thixoforming. The composite alloy shows the highest UTS which is 258.77 MPa due to the interchange of molecules and packed intermetallic status. The favourable condition in Short T6 HT improved the ultimate tensile strength with 43.8 % MPa and 75.62 % MPa percentage increment as compared to thixoforming (211.88 MPa) and as – cast (147.34 MPa) with respectively as shown in Table 4.2.

Graph YS (Figure 4.6) below showed lowest yield strength for as – cast with 82.07 MPa but improved significantly to thixoformed composite alloy to Short T6 heat treatment, 104.94 MPa to 134.36 MPa respectively. The steady increasing trend MPa in as – cast to thixoformed, 27.87%, and thixoformed to short T6 heat treatment with 28.04% proved that the evolution of microstructure as well as thermal stress between the al- matrix affect the formation of globular microstructure of silicon particles in short T6 HT that only need approximately of 5 minutes of quenching time, as the sample must undergo thixoforming process prior to T6 HT. Based on Lu et al., 2018 the results also showed that UTS and elongation percentage of Al - composite alloy were improved. The sample uses shorter overall solution treatment and reaches maximum hardness for the formation of θ – phase.

52

The tensile characteristics and ductility of an Al-A308 alloy as a function of temperature and heat treatment were studied in this study. Tensile testing was performed on the alloy as-cast, after thixoformed, and after solid solution at 540°C, accompanied by quenching and ageing at 180°C (T6). Heat treatment increased the alloy tensile strength from 147.34 MPa in the as-cast condition to 258.77 MPa in the thixoformed T6 condition, according to the study. Moreover, the alloy elongation was relatively increasing from 4.24% to 8.93% as shown in Figure 4.7 above. According to Salleh et al., in 2017, fractures in as-cast samples can be classified as brittle fractures and as – thixoformed sample showed ductile fracture. The difference between the thixoformed samples is that they are fine and well distributed dimple fractures as compared to as – cast sample with fractures on long Si particles.
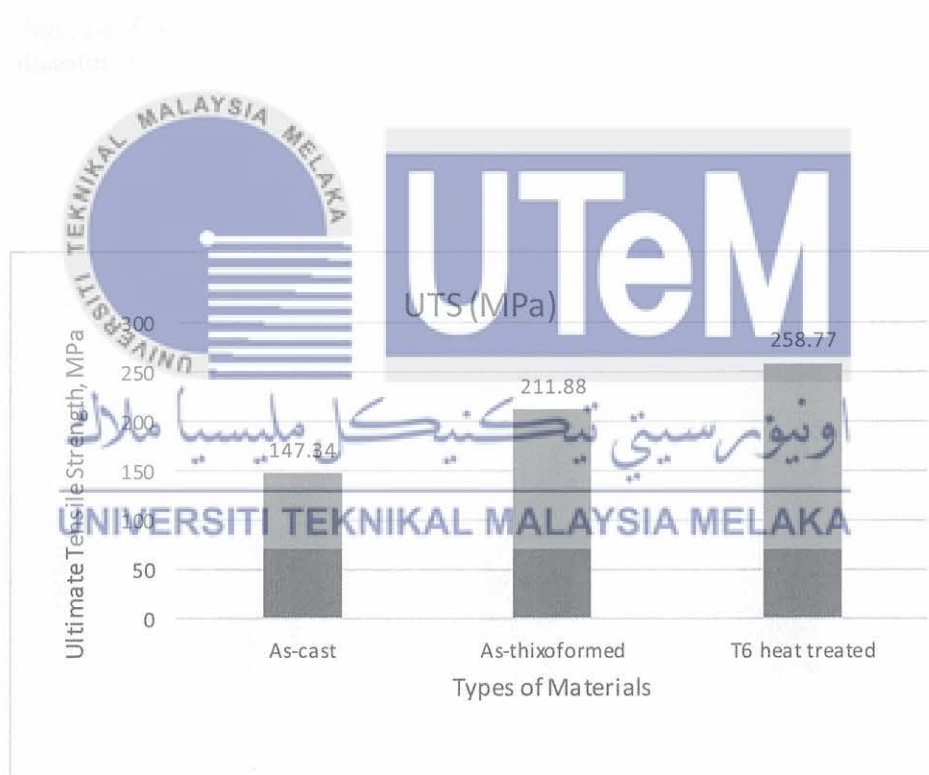
Figure 4. 5: Bar graph of Ultimate Tensile Strength (UTS) for as-cast, thixoformed and thixoformed T6 heat treated
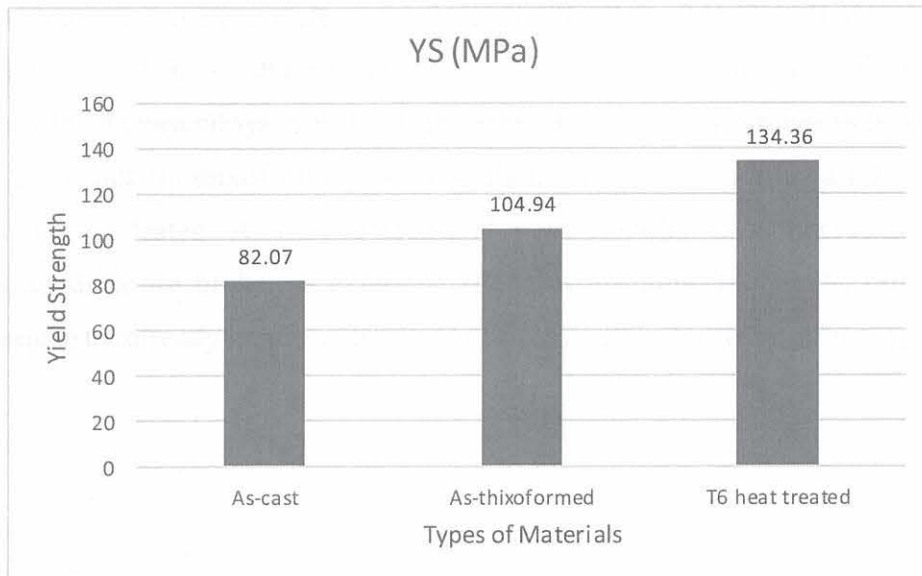
Figure 4. 6: Bar graph of Yield Strength (YS) for as-cast, thixoformed and thixoformed T6 heat treated
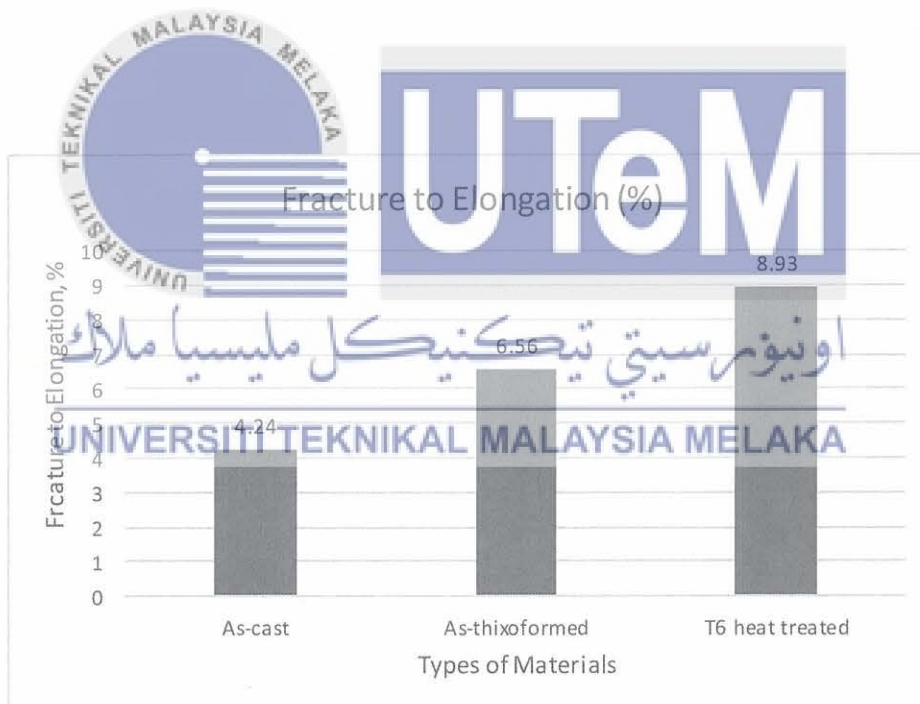
Figure 4. 7: Bar graph of Fracture to Elongation, % for as-cast, thixoformed and thixoformed T6 heat treated

The mechanical testing results for elongation of fracture, yield strength and ultimate tensile strength showed that outstanding mechanical properties were fulfilled with the short T6 heat treatment in SSM processing. This study shows that thixoformed LM21/A308 Al alloy with

54

T6 heat treatment parameters of short treatment at 540 °C for 8 hours of holding time, 4 hours of ageing at 180 °C attain better tensile strength, surface hardness than the as-thixoformed and as-cast alloys. Stir casting at 500rpm (700⁰C) for 5 minutes produce the best billet feedstock for thixoforming as primarily the irregular dendritics are broken and homogenously nucleated. A well-defined and near globular α-Al microstructure as secondary dendritic are broken is exhibited after thixoforming. T6 heat treatment adds enhancement to the already improved properties of LM21 alloy due to thixoforming process.

CHAPTER 5.0
CONCLUSION AND RECOMMENDATIONS

5.1 Conclusion

The microstructure of A308 as-cast consists of majorly dendritic arms as well as intermetallic compounds. Dendritics were the effect of stirring time during casting with the factor of stirring speed. After 5 minutes of stirring, particles were combined in higher numbers as time progressed. Mechanical stirring led to voids and porosities, which impacted to decreases in the hardness and UTS of the composite. Secondary procedures which were the thixoforming and T6 heat treatment were compulsory to reduce such effects. Thixoformed microstructures showed rosette-like and semi-globular microstructures surrounded by eutectic microconstituents attained after mechanical stirring. The thixoformed finger presents a uniform distribution of nearly globular α-Al grains. The development of the phase has apparently occurred in a semi-solid state with no evidence of deformation in the grains. The flow of the liquid phase under thixoforming pressure ought to help with the shaping of the structure to be more globule or round. Globular coalescence will increase the viscosity of the material, which leads to it being able to support its own weight and be handled in the same way as if it was solid giving the increase of the grain size due to shear. The aim of the solution treatment is to dissolve (in intermetallic states in Al- rich matrix (α-Al) and get the equilibrium state) while in quenching step, the formation of $Al2Cu$ intermetallic metastable phase is reached with the spread in α-Al solution by the help of warm water to produce superheated solid solution that will precipitated lastly in the aging step. The microstructure was globular after T6 heat treated and both the thixoforming process and T6 heat treatment had eliminated the dendritic microstructure and T6 heat treatment form a globular microstructure. In overall, the morphology properties of Thixoformed significantly improves after T6 heat treatment.

For mechanical testing, the highest hardness obtained was from the T6 heat treated sample which was 128.4 HV. While the lowest hardness value is from as-cast which is only 97.5 HV compared to 123.4 HV to thixoformed. The increased hardness of the thixoformed after T6 heat treatment sample was due to the extremely low porosity and size of alpha aluminium grains throughout the sample has increased. It is concluded that the rise in the measurement can be attributed through the precipitation of an intermetallic phase among the alpha aluminium globules in the alloys. Since the measurement shows increasing off 4.05% in hardness after the T6 heat treatment process. On top of that, the highest UTS, YS and EL% obtained are also from the thixoformed T6 heat treated sample with 258.77 MPa in Ultimate Tensile Strength, 134.36 MPa in Yield Strength and 8.93% in Elongation to Fracture. The percentage of 43.8 %, 28.04%, 36.13% were the increase percentage of T6 heat treated process from the thixoformed process respectively. T6 heat treatment leads to the best results in morphological properties as well as the mechanical analysis in general.

5.2 Recommendations

To increase the mechanical properties and morphological structure, it is recommended to add reinforcement elements. Reinforcement elements such as Carbon Nanotube (CNT). Stirring's effects have been studied extensively, not only for CNTs but also for other reinforcement materials. Load transmission, dislocations caused by thermal mismatch, and the Orowan looping system are the main strengthening mechanisms of CNT/Al composites. In order to achieve efficient interfacial bonding and effective load transfer in the areas, a good wettability between the reinforcement and matrix is required, in addition to the homogeneous distribution of the CNT. Wettability refers to the CNT's potential to wet and break down the matrix's surface tension. Furthermore, the amount of reinforcement in the matrix has a significant impact on the composites' mechanical properties. Bakr et al., for example, found a rising pattern in the hardness of CNT/A356 composite liquid state fabrication from 0.5, 1.0, and 2.5 wt percent CNT. Similarly, with 6.0 wt percent CNT, Bradbury et al. achieved the best hardness of 140 HV, and hardness began to decline beyond this proportion. The contact between the MWCNT and the matrix is widely acknowledged to play a significant impact in the composite's strength. According to Rikhtegar et al. and Chen et al., a strong interfacial connection allows for effective load distribution from the matrix to the reinforced particle.

A possible future work that is recommended is to apply Design of Experiment Taguchi for the experiment as to make it systematic by having an efficient method that engineers to study the relationship between multiple input variables or factors and key output variables or response. It is a structured approach for collecting data and making discoveries.

5.3 Sustainable Design and Development

Stir casting is among the most cost-effective methods for making metal matrix composites because of its simple structure, flexibility, and low processing costs. Reduced stirring time is necessary for a more ecologically friendly manufacturing process in stir casting, which can be accomplished by optimising various stirring elements, particularly the stirrer design and position. Increased stirring time in the AAMC stir casting manufacturing process may result in better distribution of micro-ceramics powder in the aluminium alloy matrix, but it comes at the expense of resources and energy. Much effort and money has gone into improving the mechanical properties of MMCs in recent years, but the flow pattern during stirring cannot be viewed since it takes place in closed, opaque furnaces; direct measurements are therefore risky, time-consuming, and ineffective. In addition to experimentation, statistical analysis and numerical simulation are utilised to overcome these problems. It is preferable to reduce the stirring time since the higher the stirring time, the higher the cost.

5.4 Complexity

While making this project a success, there were complexity that must be faced. Mainly, when undergoing the thixoforming process, the T308 Machine shut down many times during working. It is said that the machine had not received enough power from the source as it requires a high current to supply to the machine. With that being said, the situation made it delayed the progress of my project. Furthermore, it happened frequently when the process is almost finished. The consequence was which I sometimes had to remove the material in used to a new one because it was broken or became irregular shape. So, I had to remake the billet again by using stir casting.

For the complexity above, my solution was to start the thixoforming process when the temperature of water chiller is as low as possible.

5.5 Life-Long Learning

The knowledge gained through this study is to develop an understanding of thixoforming machine, CNC turning machine in casting formability for future technology in machining.

REFERENCES

Adediran, A. A., Akinwande, A. A., Balogun, O. A., Olorunfemi, B. J., & Saravana Kumar, & M. (123 C.E.). Optimization studies of stir casting parameters and mechanical properties of TiO 2 reinforced Al 7075 composite using response surface methodology. *Scientific Reports*, *11*. https://doi.org/10.1038/s41598-021-99168-1

Atkinson, H. V., & Liu, D. (2010). Coarsening rate of microstructure in semi-solid aluminium alloys. *Transactions of Nonferrous Metals Society of China*, *20*(9), 1672–1676. https://doi.org/10.1016/S1003-6326(09)60356-3

Bakr, A., Khattab, A., Osman, T. A., Azzam, B., & Zaki, M. (2014). *A Novel Technique for Dispersion of MWCNTs in Aluminum Alloys*, *3*(1), 2022.

Bradbury, C. R., Gomon, J. K., Kollo, L., Kwon, H., & Leparoux, M. (2014). Hardness of Multi Wall Carbon Nanotubes reinforced aluminium matrix composites. *Journal of Alloys and Compounds*, *585*, 362–367. https://doi.org/10.1016/J.JALLCOM.2013.09.142

Choi, H. J., Shin, J. H., & Bae, D. H. (2011). Grain size effect on the strengthening behavior of aluminum-based composites containing multi-walled carbon nanotubes. *Composites Science and Technology*, *71*(15), 1699–1705. https://doi.org/10.1016/J.COMPSCITECH.2011.07.013

Hanizam, H., Salleh, M. S., Omar, M. Z., & Sulong, A. B. (2019). Optimisation of mechanical stir casting parameters for fabrication of carbon nanotubes-aluminium alloy composite through Taguchi method. *Journal of Materials Research and Technology*, *8*(2), 2223–2231. https://doi.org/10.1016/j.jmrt.2019.02.008

Hashim, H., Salleh, M. S., Omar, M. Z., Sulong, A. B., & Rahman, A. A. (2021). Influence of short heat treatment on the microstructures and mechanical properties of Thixoformed aluminum alloy composite. *Jurnal Tribologi*, *28*(January), 96–104.

Li, P. B., Chen, T. J., & Qin, H. (2016). Effects of mold temperature on the microstructure and tensile properties of SiCp/2024 Al-based composites fabricated via powder

thixoforming. *Materials & Design*, *112*, 34–45. https://doi.org/10.1016/J.MATDES.2016.09.049

Lu, S. ping, Du, R., Liu, J. ping, Chen, L. can, & Wu, S. sen. (2018). A new fast heat treatment process for cast A356 alloy motorcycle wheel hubs. *China Foundry*, *15*(1), 11–16. https://doi.org/10.1007/s41230-018-7058-x

Magno, I. A. B., De Souza, F. V. A., Dos Santos Barros, A., Costa, M. O., Nascimento, J. M., De Sousa Costa, T. A. P., & Da Rocha, O. F. L. (2017). Effect of the T6 heat treatment on microhardness of a directionally solidified aluminum-based 319 alloy. *Materials Research*, *20*, 667–675. https://doi.org/10.1590/1980-5373-mr-2016-0961

Mohammed, M. N., Omar, M. Z., Salleh, M. S., Alhawari, K. S., & Kapranos, P. (2013). Semisolid Metal Processing Techniques for Nondendritic Feedstock Production. *The Scientific World Journal*, *2013*, 16. https://doi.org/10.1155/2013/752175

Peng, J. H., Tang, X. L., He, J. T., & Xu, D. Y. (2011). Effect of heat treatment on microstructure and tensile properties of A356 alloys. *Transactions of Nonferrous Metals Society of China*, *21*(9), 1950–1956. https://doi.org/10.1016/S1003-6326(11)60955-2

Prabu, S. B., Karunamoorthy, L., Kathiresan, S., & Mohan, B. (2006). Influence of stirring speed and stirring time on distribution of particles in cast metal matrix composite. *Journal of Materials Processing Technology*, *171*(2), 268–273. https://doi.org/10.1016/J.JMATPROTEC.2005.06.071

Rahman, A. A., Salleh, M. S., Othman, I. S., Yahaya, S. H., Al-Zubaidi, S. S., & Zulkifli, K. (2020). Investigation Of Mechanical & Wear Characteristics Of T6 Heat Treated Thixoformed Aluminium Alloy Composite. *Journal of Advanced Manufacturing Technology*, *14*(3), 1–14.

Song, J., She, J., Chen, D., Pan, F., Chang, Z., Wang, X., Wu, Y., Peng, L., Ding, W., Kielbus, A., Rzychon, T., Alloys, M., Resistance, C. C., Casting, S., Strength, T., Element, A., Resistance, C. C., Fujisawa, S., Yonezu, A., … Cahn, J. W. (2020). Semi-solid manufacturing process of magnesium alloys by twin-roll casting. *Journal of Magnesium and Alloys*, *8*(2), 109486. https://doi.org/10.1016/j.jma.2014.01.001

Tavitas-Medrano, F. J., Gruzleski, J. E., Samuel, F. H., Valtierra, S., & Doty, H. W. (2008). Effect of Mg and Sr-modification on the mechanical properties of 319-type

aluminum cast alloys subjected to artificial aging. *Materials Science and Engineering: A*, *480*(1–2), 356–364. https://doi.org/10.1016/J.MSEA.2007.09.002

Wallerstein, D., Riveiro, A., Val, J. del, Comesaña, R., Lusquiños, F., & Pou, J. (2021). Developments in laser welding of aluminum alloys. *Advanced Welding and Deforming*, 127–150. https://doi.org/10.1016/B978-0-12-822049-8.00005-0

Editorial Board. (2020). *Journal of PhysiC.S and Chemistry of Solids*, *144*, 109587. https://doi.org/10.1016/s0022-3697(20)31440-2

Numerical investigation of grain refinement of magnesium alloys: Effects of cooling rate ScienceDirect. (n.d.). Retrieved June 22, 2021, from https://www.sciencedirect.com/science/article/abs/pii/S0022369720302729

Atkinson, H. V. (2005). Modelling the semisolid processing of metallic alloys. In *Progress in Materials Science* (Vol. 50, Issue 3, pp. 341–412). Pergamon. https://doi.org/10.1016/j.pmatsci.2004.04.003

Cahn, J. W. (1960). Theory of crystal growth and interface motion in crystalline materials. *Acta Metallurgica*, *8*(8), 554–562. https://doi.org/10.1016/0001-6160(60)90110-3

Chang, Z., Wang, X., Wu, Y., Peng, L., & Ding, W. (2021). Review on criteria for assessing the processability of semisolid alloys. *Materials Letters*, *282*, 128835. https://doi.org/10.1016/j.matlet.2020.128835

Chayong, S., Atkinson, H. V., & Kapranos, P. (2005). Thixoforming 7075 aluminium alloys. *Materials Science and Engineering A*, *390*(1–2), 3–12. https://doi.org/10.1016/j.msea.2004.05.004

Chen, T., Xie, Z. W., Luo, Z. Z., Yang, Q., Tan, S., Wang, Y. J., & Luo, Y. M. (2014). Microstructure evolution and tensile mechanical properties of thixoformed AZ61 magnesium alloy prepared by squeeze casting. *Transactions of Nonferrous Metals Society of China (English Edition)*, *24*(11), 3421–3428. https://doi.org/10.1016/S1003-6326(14)63485-3

Chen, X., Jia, Y., Le, Q., Ning, S., Li, X., & Yu, F. (2020). The interaction between in situ grain refiner and ultrasonic treatment and its influence on the mechanical properties of

Mg–Sm–Al magnesium alloy. *Journal of Materials Research and Technology*, *9*(4), 9262–9270. https://doi.org/10.1016/j.jmrt.2020.06.044

Citation, S. (1975). Trends in Usage of Magnesium. In *Trends in Usage of Magnesium*. https://doi.org/10.17226/21318

de Paiva, J. A. C., Graça, M. P. F., Monteiro, J., Macedo, M. A., & Valente, M. A. (2009). Spectroscopy studies of NiFe2O4 nanosized powders obtained using coconut water. *Journal of Alloys and Compounds*, *485*(1–2), 637–641. https://doi.org/10.1016/j.jallcom.2009.06.052

Dong, J., Cui, J. Z., Le, Q. C., & Lu, G. M. (2003). Liquidus semi - continous casting, reheating and thixoforming of a wrought aluminum alloy 7075. *Materials Science and Engineering A*, *345*(1–2), 234–242. https://doi.org/10.1016/S0921-5093(02)00473-2

Gebelin, J. C., Suéry, M., & Favier, D. (1999). Characterisation of the rheological behaviour in the semi-solid state of grain-refined AZ91 magnesium alloys. *Materials Science and Engineering A*, *272*(1), 134–144. https://doi.org/10.1016/S0921-5093(99)00467-0

GECU, R., ACAR, S., KISASOZ, A., ALTUG GULER, K., & KARAASLAN, A. (2018). Influence of T6 heat treatment on A356 and A380 aluminium alloys manufactured by thixoforging combined with low superheat casting. *Transactions of Nonferrous Metals Society of China (English Edition)*, *28*(3), 385–392. https://doi.org/10.1016/S1003-6326(18)64672-2

Goel, R., Jha, R., & Ravikant, C. (2020). Investigating the structural, electrochemical, and optical properties of p-type spherical nickel oxide (NiO) nanoparticles. *Journal of Phys. C. S and Chemistry of Solids*, *144*. https://doi.org/10.1016/j.jpC.S.2020.109488

Grong, & Shercliff, H. R. (2002). Microstructural modelling in metals processing. In *Progress in Materials Science* (Vol. 47, Issue 2, pp. 163–282). Pergamon. https://doi.org/10.1016/S0079-6425(00)00004-9

Jiang, J., Wang, Y., Xiao, G., & Nie, X. (2016). Comparison of microstructural evolution of 7075 aluminum alloy fabricated by SIMA and RAP. *Journal of Materials*

63

Processing Technology, 238, 361–372. https://doi.org/10.1016/j.jmatprotec.2016.06.020

Karthik, A., Karunanithi, R., Srinivasan, S. A., & Prashanth, M. (2019). The optimization of squeeze casting process parameter for AA2219 alloy by using the Taguchi method. *Materials Today: Proceedings*, 27, 2556–2561. https://doi.org/10.1016/j.matpr.2019.10.136

Le, T., Wei, Q., Wang, J., Jin, P., Chen, M., & Ma, J. (2020). Effect of different casting techniques on the microstructure and mechanical properties of AE44-2 magnesium alloy. *Materials Research Express*, 7(11). https://doi.org/10.1088/2053-1591/abc721

Li, H. T., Wang, Y., & Fan, Z. (2012). Mechanisms of enhanced heterogeneous nucleation during solidification in binary Al-Mg alloys. *Acta Materialia*, 60(4), 1528–1537. https://doi.org/10.1016/j.actamat.2011.11.044

Liu, B., Yang, Y., Zhang, Y., Du, H., Hou, L., & Wei, Y. (2020). Investigation of rapidly decomposable AZ91–RE–xCu (x=0, 1, 2, 3, 4) alloys for petroleum fracturing balls. *Journal of Physics and Chemistry of Solids*, 144. https://doi.org/10.1016/j.jpcs.2020.109499

Liu, D. R., Zhao, H., & Wang, L. (2020). Numerical investigation of grain refinement of magnesium alloys: Effects of cooling rate. *Journal of Physics and Chemistry of Solids*, 144, 109486. https://doi.org/10.1016/j.jpcs.2020.109486

Liu, X., Shan, D., Song, Y., & Han, E. hou. (2017). Influence of yttrium element on the corrosion behaviors of Mg–Y binary magnesium alloy. *Journal of Magnesium and Alloys*, 5(1), 26–34. https://doi.org/10.1016/j.jma.2016.12.002

Lu, D. S., Li, W. S., Jiang, X., Tan, C. L., & Zeng, R. H. (2009). Magnetic field assisted chemical reduction preparation of Co-B alloys as anode materials for alkaline secondary battery. *Journal of Alloys and Compounds*, 485(1–2), 621–626. https://doi.org/10.1016/j.jallcom.2009.06.060

Lü, Y., Wang, Q., Zeng, X., Ding, W., Zhai, C., & Zhu, Y. (2000). Effects of rare earths on the microstructure, properties and fracture behavior of Mg-Al alloys. *Materials*

Science and Engineering, 278(1–2), 66–76. https://doi.org/10.1016/S0921-5093(99)00604-8

Luo, S., Chen, Q., & Zhao, Z. (2009). An investigation of microstructure evolution of RAP processed ZK60 magnesium alloy. Materials Science and Engineering, 501(1–2), 146–152. https://doi.org/10.1016/j.msea.2008.09.059

Luo, S., Chen, Q., & Zhao, Z. (2009). Effects of processing parameters on the microstructure of ECAE-formed AZ91D magnesium alloy in the semi-solid state. Journal of Alloys and Compounds, 477(1–2), 602–607. https://doi.org/10.1016/j.jallcom.2008.10.101

Marsavina, L., Iacoviello, F., Dan Pirvulescu, L., Di Cocco, V., & Rusu, L. (2019). Engineering prediction of fatigue strength for AM50 magnesium alloys. International Journal of Fatigue, 127, 10–15. https://doi.org/10.1016/j.ijfatigue.2019.05.028

Mohammed, M. N., Omar, M. Z., Salleh, M. S., Alhawari, K. S., & Kapranos, P. (2013). Semisolid Metal Processing Techniques for Nondendritic Feedstock Production. The Scientific World Journal, 2013, 16. https://doi.org/10.1155/2013/752175

Mordike, B. L., & Ebert, T. (2001). Magnesium Properties - applications - potential. Materials Science and Engineering, 302(1), 37–45. https://doi.org/10.1016/S0921-5093(00)01351-4

Mordike, B. L., & Ebert, T. (2001). Magnesium Properties - applications - potential. Materials Science and Engineering, 302(1), 37–45. https://doi.org/10.1016/S0921-5093(00)01351-4

Menargues, S., Martín, E., Baile, M. T., & Picas, J. A. (2015). New short T6 heat treatments for aluminium silicon alloys obtained by semisolid forming. Materials Science and Engineering: A, 621, 236–242. https://doi.org/https://doi.org/10.1016/j.msea.2014.10.078

Papenberg, N. P., Gneiger, S., Weißensteiner, I., Uggowitzer, P. J., & Pogatscher, S. (n.d.). materials Mg Alloys for Forging Applications A Review https://doi.org/10.3390/ma13040985

65

Pu, Z., Wang, L., & Liu, D. R. (2020). Numerical modeling of grain refinement during solidification of Mg-4Y-3Nd (wt.%) alloy via mesh-anisotropy reduction algorithm. *Materials Today Communications*, 25. https://doi.org/10.1016/j.mtcomm.2020.101679

Song, J., She, J., Chen, D., & Pan, F. (2020). Latest research advances on magnesium and magnesium alloys worldwide. In *Journal of Magnesium and Alloys* (Vol. 8, Issue 1, pp. 1–41). National Engg. Reaserch Center for Magnesium Alloys. https://doi.org/10.1016/j.jma.2020.02.003

Song, J., She, J., Chen, D., Pan, F., Chang, Z., Wang, X., Wu, Y., Peng, L., Ding, W., Kielbus, A., Rzychon, T., Alloys, M., Resistance, C. C., Casting, S., Strength, T., Element, A., Resistance, C. C., Fujisawa, S., Yonezu, A., … Cahn, J. W. (2020). Semi-solid manufacturing process of magnesium alloys by twin-roll casting. *Journal of Magnesium and Alloys*, 8(2), 109486. https://doi.org/10.1016/j.jma.2014.01.001

Tong, X., You, G., Luo, J., Ebrahimi, M., & Wu, G. (2021). Rapid cooling effect during solidification on macro- and micro-segregation of as-cast Mg–Gd alloy. *Progress in Natural Science: Materials International*, 31(1), 68–76. https://doi.org/10.1016/j.pnsc.2020.09.005

Wang, Y., Liu, G., & Fan, Z. (2006). Microstructural evolution of rheo-diecast AZ91D magnesium alloy during heat treatment. *Acta Materialia*, 54(3), 689–699. https://doi.org/10.1016/j.actamat.2005.09.033

Wu, G., Fan, Y., Gao, H., Zhai, C., & Zhu, Y. P. (2005). The effect of Ca and rare earth elements on the microstructure, mechanical properties and corrosion behavior of AZ91D. *Materials Science and Engineering A*, 408(1–2), 255–263. https://doi.org/10.1016/j.msea.2005.08.011

Xia, K., & Tausig, G. (1998). Liquidus casting of a wrought aluminum alloy 2618 for thixoforming. *Materials Science and Engineering A*, 246(1–2), 1–10. https://doi.org/10.1016/s0921-5093(97)00758-2

Xu, T., Yang, Y., Peng, X., Song, J., & Pan, F. (2019). Overview of advancement and development trend on magnesium alloy. *Journal of Magnesium and Alloys*, 7(3), 536–544. https://doi.org/10.1016/j.jma.2019.08.001

Yadav, D. K., & Chakrabarty, I. (2020). Effect of cooling slope casting and partial remelting treatment on microstructure and mechanical properties of A319-xMg2Si In-Situ composites. *Materials Science and Engineering A*, 791, 139790. https://doi.org/10.1016/j.msea.2020.139790

Zhang, J., Niu, X., Qiu, X., Liu, K., Nan, C., Tang, D., & Meng, J. (2009). Effect of yttrium-rich misch metal on the microstructures, mechanical properties and corrosion behavior of die cast AZ91 alloy. *Journal of Alloys and Compounds*, 471(1–2), 322–330. https://doi.org/10.1016/j.jallcom.2008.03.089

ZHANG, S. qing, CHEN, T. jun, CHENG, F. liang, & LI, L. liang. (2016). Microstructural evolution and phase transformation during partial remelting of in-situ Mg2Sip/AM60B composite. *Transactions of Nonferrous Metals Society of China (English Edition)*, 26(6), 1564–1573. https://doi.org/10.1016/S1003-6326(16)64262-0

Zhao, W., Wang, J., Weiyang, J., Qiao, B., Wang, Y., Li, Y., & Jiang, D. (2020). A novel biodegradable Mg-1Zn-0.5Sn alloy: Mechanical properties, corrosion behavior, biocompatibility, and antibacterial activity. *Journal of Magnesium and Alloys*, 8(2), 374–386. https://doi.org/10.1016/j.jma.2020.02.008

Zhao, Z., Chen, Q., Chao, H., & Huang, S. (2010). Microstructural evolution and tensile mechanical properties of thixoforged ZK60-Y magnesium alloys produced by two different routes. *Materials and Design*, 31(4), 1906–1916. https://doi.org/10.1016/j.matdes.2009.10.056

Zhao, Z., Chen, Q., Hu, C., Huang, S., & Wang, Y. (2009). Near-liquidus forging, partial remelting and thixoforging of an AZ91D + Y magnesium alloy. *Journal of Alloys and Compounds*, 485(1–2), 627–636. https://doi.org/10.1016/j.jallcom.2009.06.053

Zhao, Z., Chen, Q., Hu, C., Huang, S., & Wang, Y. (2009). Near-liquidus forging, partial remelting and thixoforging of an AZ91D + Y magnesium alloy. *Journal of Alloys and Compounds*, 485(1–2), 627–636. https://doi.org/10.1016/j.jallcom.2009.06.053

Zhao, Z., Chen, Q., Hu, C., Huang, S., & Wang, Y. (2009). Near-liquidus forging, partial remelting and thixoforging of an AZ91D + Y magnesium alloy. *Journal of Alloys and Compounds*, *485*(1–2), 627–636. https://doi.org/10.1016/j.jallcom.2009.06.053

Zhao, Z., Chen, Q., Hu, C., Huang, S., & Wang, Y. (2009). Near-liquidus forging, partial remelting and thixoforging of an AZ91D + Y magnesium alloy. *Journal of Alloys and Compounds*, *485*(1–2), 627–636. https://doi.org/10.1016/j.jallcom.2009.06.053

Zheng, M. Y., Wu, K., Liang, M., Kamado, S., & Kojima, Y. (2004). The effect of thermal exposure on the interface and mechanical properties of Al18B4O33w/AZ91 magnesium matrix composite. *Materials Science and Engineering*, *347*(1–2), 66–74. https://doi.org/10.1016/j.msea.2003.09.085